Chemosphere 380 (2025) 144435

Contents lists available at ScienceDirect

Chemosphere

journal homepage: www.elsevier.com/locate/chemosphere

Remediating heavy metal-contaminated soil through invasive alien plant-derived biochar and stinging nettle powder

Alex Ceriani [a,*], Yassine Chafik [b], Alessio Miali [a], Sylvain Bourgerie [b], Michele Dalle Fratte [a], Bruno E.L. Cerabolini [a], Domenico Morabito [b], Antonio Montagnoli [a,**]

[a] University of Insubria, Department of Biotechnology and Life Science, Via Dunant 3, 21100, Varese, Italy
[b] University of Orléans, P2E-EA1207, INRAE USC1328, Rue de Chartres, Orléans, 45067 Cedex 2, France

HIGHLIGHTS

- *Solidago* biochar alone and *Ailanthus* biochar with *Urtica* powder reduced Pb mobility.
- Invasive alien plants species biochar and *Urtica* powder increased As mobility.
- Amendments improved *P. vulgaris* development and fine root morphological traits.
- Amendments combination increased soil enzymatic activities.
- IAPS-derived biochar proves effective for contaminated soil management.

GRAPHICAL ABSTRACT

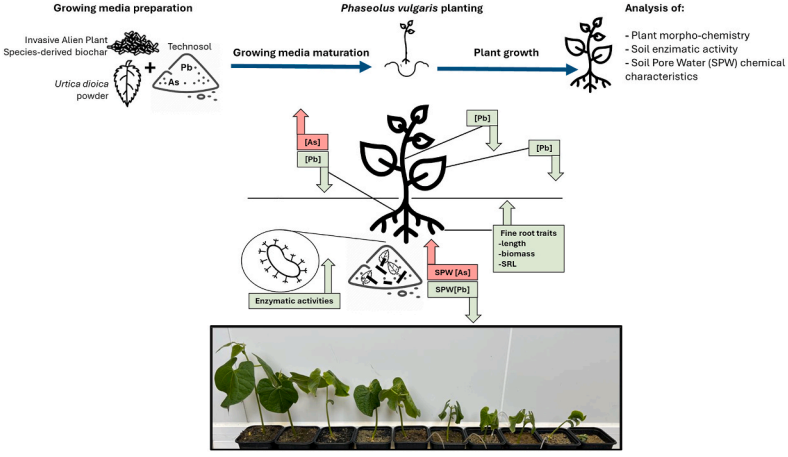

ARTICLE INFO

Keywords:
Ailanthus altissima
Solidago gigantea
Arsenic
Lead
Phytostabilization
Root traits
Soil pore water

ABSTRACT

Invasive alien plant species (IAPS) threaten ecosystem integrity worldwide. IAPS eradication is expensive, and their biomass is considered waste. Producing biochar from IAPS biomasses could turn waste into a resource. At the same time, this material could be used to remediate polluted soils. Also, using widespread native weeds, such as *Urtica dioica* (*U*), as an additional amendment could further improve soil remediation. In a phytoremediation experiment, we applied biochar produced from two widespread IAPS' biomass, i.e. *Ailanthus altissima* (Mill.) (BA) and *Solidago gigantea* Aiton (BS), at different rates (2 % and 5 % w/w) together with *Urtica dioica* L. powder (*U*) (2 % w/w) in an Arsenic (As) and Lead (Pb)-contaminated soil, using *Phaseolus vulgaris* L. as an indicator plant species. We measured the amendment's effects on soil pore water (SPW) properties, plant and fine root development, and soil enzymatic activities. When BS was added alone, and when BA was combined with *U* SPW's pH

* Corresponding author. Via Monte Generoso 71, Varese, 21100, Italy.
** Corresponding author. Via Monte Generoso 71, Varese, 21100, Italy.
E-mail addresses: alex.ceriani@uninsubria.it (A. Ceriani), antonio.montagnoli@uninsubria.it (A. Montagnoli).

https://doi.org/10.1016/j.chemosphere.2025.144435
Received 19 December 2024; Received in revised form 15 April 2025; Accepted 19 April 2025
Available online 3 May 2025

and electrical conductivity (EC) increased and [Pb] diminished, which augmented plant growth and reduced Pb uptake. Combining the biochar types and *U* increased the soil's enzymatic activities, fine root length, biomass, and specific root length. Finally, both biochar types with *U* increased As mobility in SPW, leading to higher plant uptake in roots, although without translocation to aboveground organs. Our findings contribute to developing cost-effective and environmentally sustainable practices for managing polluted soil. Simultaneously, they tackle the problem of IAPS, which can be used in the future to provide guidelines for policymakers.

List of abbreviations

As =	Arsenic
BA =	Biochar derived from *Ailanthus altissima*
BS =	Biochar derived from *Solidago gigantea*
CEC =	Cation exchange capacity
D+14 =	sampling after two weeks from the sewing of seeds
D0 =	seed sewing
D-14 =	first sampling time
EC =	electrical conductivity
IAPS =	Invasive alien plant species
Pb =	Lead
SPW =	Soil pore water
U =	*Urtica dioica* powder

1. Introduction

Invasive alien plant species (IAPS) threaten ecosystem functioning and services worldwide, impacting biodiversity. EU law (1143/2014) requires IAPS management and eradication, involving careful planning and multiple costly interventions due to their wide distribution and rapid regrowth (Haubrock et al., 2021). Using IAPS biomass as feedstock for different applications could enhance IAPS management efforts (Ceriani et al., 2023). IAPS biomass is an overlooked feedstock for producing biochar (Wang et al., 2021; Ceriani et al., 2024), i.e. the carbon-rich solid residue derived from pyrolyzing biomass under limited oxygen conditions. Biochar properties depend on feedstock characteristics and pyrolysis conditions (Weber & Quicker 2018), and it is recognized as an environmentally friendly and carbon-negative material (Ippolito et al., 2020). Thus, evaluating the potential IAPS-derived biochar applications is essential to achieve sustainable management practices.

Biochar stabilizes soil pollutants (Sanaei et al., 2023), such as heavy metals, and is a valuable tool for *in-situ* remediation (Feng et al., 2021). Applying biochar to acidic heavy-metal-polluted soils decreases metal mobility, bioavailability, and plant uptake (Chen et al., 2018). Biochar increases the soil water-holding capacity, pH, and cation exchange capacity (CEC) and soil pore water (SPW), making it an asset for phytoremediation (Wu et al., 2024).

The effectiveness of biochar in the soil varies with application rates, feedstock, production processes, and soil properties (Xiang et al., 2017; Chen et al., 2018; Beatrice et al., 2023). Also, biochar alone may not supply enough bioavailable nutrients in heavily polluted soils, and it can be combined with amendments such as compost, mulch, or green manure for enhanced efficiency (Fischer and Glaser, 2012; Nandillon et al., 2019b; Sharifan and Ma, 2021; Dalle Fratte et al., 2022; Lebrun et al., 2023).

Hence, IAPS can be utilized as biochar, which helps manage their spread and valorize their biomass, which is considered waste. Additionally, widely distributed herbaceous perennial plants like *Urtica dioica* L. (known as stinging nettle), which thrive in nutrient-rich and polluted soils (Viotti et al., 2022), could serve as an affordable and easily accessible amendment rich in macronutrients to be incorporated with IAPS-derived biochar. This may further enhance plant growth and improve phytoremediation efforts (Viotti et al., 2022). However, the effectiveness of incorporating IAPS-derived biochar and *Urtica* amendments in heavy-metal polluted soils is largely unknown (Beesley et al., 2010), necessitating detailed analysis. The innovative aspects of this study involve using biochar produced from the biomass of two prevalent IAPS in Europe: the woody *Ailanthus altissima* (Mill.) S. and the herbaceous *Solidago gigantea* A. These two biochar types have been characterized for their ability to adsorb Pb and serve as soil amendments, respectively (Ceriani et al., 2024). This work presents a novel approach by complementing IAPS-derived biochar with nettle powder as a sustainable soil amendment. This nettle powder can be considered green manure derived from cost-effective biomass and may work synergistically with biochar to address the complexities of soil pollution. This strategy contributes to establishing a circular and sustainable approach to phytoremediation.

Biochar and different amendments can also boost soil microbial activity (Jia et al., 2017; Arif et al., 2018). Soil enzymatic activities can be indicators of these changes, responding to alterations in the edaphic environment (Paz-Ferreiro et al., 2012; LeBrun et al., 2021). The improved soil physical, chemical, and microbial conditions influence root growth (Xiang et al., 2017), increasing plant phytoremediation efficiency (Wang et al., 2024). Interestingly, biochar affects root traits differently: Xiang et al. (2017), observed increases in root biomass, whereas Biederman and Harpole (2013) reported no significant effects. These variations might stem from analyzing different fractions of the root system, i.e., the entire system or only fine roots (under 2 mm in diameter). Fine roots are crucial for water and nutrient absorption/-transport and respond rapidly to environmental changes (Montagnoli et al., 2021). They are divided into fibrous roots, with lower diameters that absorb these resources, and pioneer roots, with larger diameters that transport them (Ostonen et al., 2007; Polverigiani et al., 2011). Biochar field applications have shown reduced fibrous root development (Baronti et al., 2022; Beatrice et al., 2024) or that there were no differences in root traits compared to controls (Baronti et al., 2022); this may be due to improved soil conditions reducing the need to forage. However, no clear trend in root responses to biochar application is evident, with some pot experiments showing increased root traits (Simiele et al., 2022) while others confirmed field observations (Baronti et al., 2024). The response of fine roots to polluted soils, particularly with added biochar and amendments, has not been extensively studied (Wang et al., 2024). Investigating fine root responses in phytoremediation with IAPS-derived biochar and *Urtica* powder (*U*) would add insights into *in-situ* remediation effectiveness. Indeed, to the best of our knowledge, few studies have focused on using IAPS-derived biochar in heavy-metal polluted soils (Wang et al., 2024b), especially in combination with another amendment, such as one deriving from a widespread native weed, such as *U*.

Hence, the project's research objective was to investigate the remediation of lead (Pb) and arsenic (As) polluted soil using biochar from two widespread IAPS in Europe: *Ailanthus altissima*. and *Solidago gigantea*.

Based on previous findings (Ceriani et al., 2024), we hypothesize that, (*i*) *A. altissima*-derived biochar (BA) would reduce metal(loids)' concentration in soil pore water, (*ii*) *S. gigantea*-derived biochar (BS) would increase plant development, and (*iii*) adding *U* powder to the technosol-biochar mixture would increase the biochar's effects further improving the technosol characteristics.

To test our hypotheses, the IAPS-derived biochar types were added at

two concentrations, alone or with *U*, to a multi-heavy metal technosol using *Phaseolus vulgaris* L. as an indicator of heavy metal toxicity (Kumpiene et al., 2014). We measured the amendments' effects on: *i*) SPW properties (pH, EC, [As], [Pb], anion and cation concentration), *ii*) above- and below-ground *P. vulgaris* growth, fine-root morphological traits, and metal(loids) accumulation, and *iii*) soil enzymatic activities.

2. Materials and methods

2.1. Soil collection and characterization

We collected technosol from Saint-Pierre-le-Chastel in the former silver-lead mining district of Pontgibaud, France. Applying a composite methodology in the second settling pond within a 2 × 2 m plot, the uppermost 20 cm soil layer was sampled with a steel shovel and transferred into polyethylene bags. Specifically, we collected multiple soil samples and mixed them to create a single, representative, and composite sample. The soil was air-dried. pH and electrical conductivity (EC) were determined using a pH-EC meter (Seven Excellence, Mettler-Toledo AG, Switzerland) (see LeBrun et al., 2022). To determine pseudo-total metal(loid) concentrations [As] and [Pb], 0.2 g of soil were mixed with a 1:3 (v/v) solution of HNO_3 65 % and HCl 37 %. Were digested using a pressurized vacuum microwave system (Multiwave 3000, Anton Paar GmbH, Germany). Samples were collected in a 50 mL flask, brought to 25 mL with ultra-pure water, and filtered on a 0.45-µm nitrocellulose membrane for the ICP-AES measurements (ULTIMA 2, HORIBA, Labcompare, San Francisco, USA). CRM recovery (%) was calculated as the ratio between measured concentration to standard concentration × 100. Pb recovery was 101 %, As recovery was 98 %.

2.2. Biochar and Urtica dioica production and characterization

Biomasses of *Ailanthus altissima* and *Solidago gigantea* were collected during July 2023, chipped (~7 cm^2; GeoTech PCS70L), dried for 2 weeks at 25 °C and milled through a 4 mm sieve (mill Retsch SM 300). Biochar was prepared through slow-pyrolysis at 550 °C with a residence time of 45 min (heating rate of 20 °C min^{-1}) under nitrogen flow (ReCord, Scarperia e San Piero, Italy) (Ceriani et al., 2024). Commercial powdered *U. dioica* (Orties broyées Algoflash naturasol) (*U*) was used as the other amendment. Biochar and *U*'s pH and EC were measured (see above). Amendments and technosol's CHN content were determined with FlashEA 1112 series CHNS analyzer (Thermo-Scientific) (Ceriani et al., 2023).

2.3. SEM and EDS biochar analysis

0.1 g of each biochar was added in 10 mL Milli-Q water solution with 1 g L^{-1} of Pb^{2+}, As^{3+}, and As^{5+}, using $Pb(NO_3)_2$, KH_2AsO_4, and $Na_2HAsO_4{\cdot}7H_2O$ for the three solutions. The mixtures were shaken at 200 rpm for 24 h. Biochar was collected filtering the solutions and letting them dry for 48 h. Samples were placed on a double-faced adhesive and coated with graphite carbon. Surface morphology was observed using a scanning electron microscope (SEM, Model IT800SHL, JOEL, USA) at 5 kV. Metal localization and semi-quantitative elemental composition were obtained using Energy-dispersive X-ray spectroscopy (EDS) with ten analyses in different areas for each particle to assess measurement repeatability.

2.4. Experimental design and set-up

Phaseolus vulgaris L. Contender (early variety) seeds were obtained by "Les doights verts" (Carbon-Blanc—France).

The growing media was differently modulated in weight proportion to a final mass of 550 g.

(i) Pontgibaud technosol (PG) alone (100 %) (control);
(ii) Each biochar obtained from *A. altissima* (BA), and *S. gigantea* (BS) was mixed with the soil at 2 % and 5 % (PG-BA2, PG-BA5, PG-BS2, PG-BS5)
(iii) powdered *U. dioica* (*U*) at 2 % was mixed with the soil alone (PG-*U*) and with the soil and biochar at 2 % and 5 % (PG-*U*-BA2, PG-*U*-BA5, PG-*U*-BS2, PG-BS5);

From the prepared growing media, ten different treatments were obtained.

- Control (PG)
- BA at 2 and 5 % (PG-BA2, PG-BA5),
- BS at 2 and 5 % (PG-BS2, PG-BS5)
- Soil and *U* at 2 % (PG-*U*)
- Soil and *U* at 2 % combined with
  - o BA at 2 and 5 % (PG-*U*-BA2, PG-*U*-BA5), and
  - o BS at 2 and 5 % (PG-*U*-BS2, PG-BS5)

The mixtures stabilized for two weeks before the seedlings were planted. *P. vulgaris* seeds germinated between damp laboratory paper in a dark culture chamber at 20 (±5) °C. After three days, the most uniform seedlings were placed in individual 9 x 9 × 9 cm plastic pots.

The plants were grown for two weeks in a culture chamber (20 ± 5 °C), with 800 µmol m^{-2} s^{-1} light intensity and a 16/8 h light/dark photoperiod. Pots were maintained at field capacity with tap water.

Each treatment had.

- five replicas for plant analysis (n = 5)
- four replicas for Soil Pore Water (SPW) and root morphological analysis (n = 4).

2.5. Soil pore water (SPW) analysis

Soil Pore Water (SPW) was collected using soil moisture samplers (Rhizon, model MOM) at a 45° angle in the pots, in four replicates at three key time-points: (i) after soil mixture preparation (D-14), (ii) when seeds were planted (D0), and (iii) at the end of the experiment (D+14). SPW samples were analyzed for pH and EC (see above), anion and cation concentrations with Dionex aquion Ion Chromatography System (Thermo Scientific, USA), and total dissolved [As] and [Pb] by ICP-AES.

2.6. Plant analysis

The five most developed *P. vulgaris* plants were harvested (D+14). Leaves and stems were rinsed. Roots were washed to remove soil and biochar particles. Organs were oven-dried (40 °C for 72 h), to measure dry matter. The dried organs were ground and digested using the pressurized vacuum microwave (see above) for metal(loid) concentrations (ICP-AES).

2.7. Root morphology

Root samples were immersed in water to avoid drying and shrinkage and scanned at 800 dpi with a calibrated flatbed scanner with a transparency unit (Epson Expression 10,000 XL) and oven-dried (70 °C until constant weight). The images were analyzed with WinRhizo Pro V. 2007d software (Regent Instruments Inc., Quebec, Canada). To calculate fine root length (cm), biomass (g), and the specific root length (SRL; m g^{-1}) for three diameter classes (<0.5, 0.5–1.0, 1.0–2.0 mm).

2.8. Soil enzymatic activities analysis

After harvesting the plants, soil samples (2 g from each treatment pot) were pooled and air-dried for 72 h. Six enzymatic activities were measured in three replicates: alkaline phosphatase (AlP), acidic phosphatase (AcP), fluorescein diacetate (FDA) hydrolysis, β-glucosidase

(βG), dehydrogenase (DH), and urease (Ur). For AcP, AlP, FDA, and βG, see Lebrun et al. (2021). For DH, see Parven et al. (2025). For Ur, see Cordero et al. (2019). Spectrophotometer measurements (SpectroStar^{Nano} BMGLabtech, Champigny-sur-Marne, France) were made at 690 nm. Results were expressed using the geometric enzymatic mean (GMEA): GMEA = $(AlP \times AcP \times FDA \times \beta G \times DH \times Ur)^{1/6}$ (Paz-Ferreiro et al., 2012).

2.9. Statistical analysis

Statistical analysis was performed using R Studio software (R Core Team, 2022). We checked for data's unimodal distribution using the function "Shapiro.test" from the "stats" base R package (Shapiro and Wilk, 1965). Data that were not normally distributed were square-root transformed to ensure normal distributions and equal variances to allow the use of parametric statistics (ANOVA). ANOVA tests were performed using the "aov" function from the "stats" package. We applied Tukey's post-hoc test to compare differences among the treatments with the "TukeyHSD" function from the "Agricolae" package (de Mendiburu, 2023). To determine the effect of times, root diameter classes, and soil amendment on SPW properties and root traits, a two-way ANOVA was performed using the function "aov2" from the "stats" package, followed by Tukey's post-hoc test.

3. Results

3.1. Soil, biochar, and U. dioica characteristics

The Pontgibaud technosol has an acidic pH of 5.19 and low electrical conductivity (EC) (119.9 μS cm^{-1}), with lead (Pb) and arsenic (As) concentrations of 11608.75 mg kg^{-1} and 568.67 mg kg^{-1}, respectively (Table 1). In contrast, BS's pH was 11.65, BA's 8.83, and U's 7.15. *U* also has the highest EC at 9268.87 μS cm^{-1}, followed by BS at 6672.07 μS cm^{-1} and BA at 604.96 μS cm^{-1}. BA contained the most carbon at 84.51 %, BS at 74.63 %, *U* at 37.56 %, and PG had the lowest value (Table 1). *U* also has the highest total nitrogen content at 3.27 %, compared to BS (0.95 %) and BA (0.75 %). Hydrogen content in *U* was highest at 5.32 %, followed by BA at 2.52 %, BS at 2.14 %, and PG (Table 1).

3.2. Biochar SEM-EDS spectra

SEM images reveal the remanence of biomass vascular structures (Fig. 1a; 1d), on which SEM-EDS analysis of the particles was carried out (Fig. 1b; 1e). The EDS spectrum revealed the presence of C, O, and Pb, the latter representing most of the identified elements of BA (86.9 %) and BS (92.9 %) (Fig. 1c; 1f). None of the obtained EDS spectra revealed the presence of As.

Table 1
Properties of the Pontgibaud technosol and properties of the amendments (pH, EC, C, N, H and S). Values represent the mean of 3 replicas (n = 3) ± SE. Letters indicate post-hoc comparison at $p < 0.05$.

	PG	BA	BS	*U*
pH	5.19 ± 0.05 **d**	8.83 ± 0.19 **b**	11.65 ± 0.07 **a**	7.15 ± 0.01 **c**
EC (μS cm^{-1})	119.9 ± 8.64 **d**	604.96 ± 35.38 **c**	6672.07 ± 251.16**b**	9268.87 ± 345.25**a**
As (mg kg^{-1})	568.67 ± 40.44	b.d.l.	b.d.l.	b.d.l.
Pb (mg kg^{-1})	11608.75 ± 58.77	b.d.l.	b.d.l.	b.d.l.
C (%)	0.24 **d**	84.51 **a**	74.63 **b**	37.56 **c**
H (%)	0.18 **d**	2.52 **b**	2.14 **c**	5.32 **a**
N (%)	b.d.l.	0.75 **c**	0.95 **b**	3.27 **a**

3.3. Soil pore water (SPW) characteristics (pH, EC, anions, cations, and toxic elements)

Throughout the experiment, the pH of the control (PG) was the lowest (Fig. 2a). At D-14 without *U*, PG-BS5 had the highest pH (Fig. 2a). In treatments with biochar and *U*, all pH values were more alkaline than PG-*U*, except for PG-*U*-BA2. The highest pH at D-14 was in PG-*U*-BS5 (Fig. 2a). Without *U*, the pattern observed at D-14 was identical to that at D0. At D0, treatments with *U* showed few statistical differences, with PG-*U* having the lowest value (Fig. 2a). At D+14, in treatments without *U*, PG-BS5 had the highest value. In treatments with *U*, PG-*U*-BS5 had the highest pH (Fig. 2a). The pH increased from D-14 to D+14, with significant changes only in PG-BA5 and PG-BS2 in treatments without *U* (Fig. 2a). With *U*, the pH increased significantly with BA treatments and in PG-*U* at D0 and D +14 compared to D-14 (Fig. 2a). There was a significant *U* effect throughout the experiment, resulting in higher pH values (Table 2). Concerning the dose effect, without *U*, the 5 % application determined significant increases at D+14, with *U*, it was significant at D0 and D+14 (Table 2). Without *U*, the biochar type affected pH at all sampling times, where BS increased pH values. In the presence of *U*, BS only raised pH at D-14 (Table 2).

At D-14 without *U*, PG-BS5 exhibited the highest EC, and treatments with BA showed values comparable to PG (Fig. 2b). With *U*, BS treatments showed the highest EC (Fig. 2b). Without *U*, the patterns at D-14, D0, and D +14 were similar. The pattern at D0 and D +14 with *U* was similar to D-14, with BS treatments having the highest EC. EC increased in treatments without *U* (from D-14 to D+14) in PG, PG-BA2, PG-BA5, and PG-BS5 (Fig. 2b). With *U*, EC decreased compared to D-14, especially in BA treatments (Fig. 2b). There was a significant *U* effect at all sampling times: EC was higher with *U* (Table 2). Without *U*, a dose effect was measured at D+14, the 5 % biochar application increased EC. The biochar type affected EC at all sampling times, regardless of *U*, where BS determined the highest EC (Table 2).

Three anions and Arsenic (As), the toxic oxyanion), were measured throughout the experiment: Chloride (Cl^-), Nitrate (NO_3^-), and Sulphate (SO_4^{2-}). At D −14, without *U*, the lowest [Cl^-] was observed in PG, PG-BA2, and PG-BA5, while the highest was PG-BS5. With *U*, the lowest values were in PG-*U* and PG-*U*-BA5, and the highest were in PG-*U*-BS5. Similar findings were observed at D0 and D+14 (Fig. 3a). Only PG showed different concentrations at different sampling times, increasing between D-14 and D+14 (Fig. 3a). At all sampling times, [Cl^-] was significantly higher with *U* addition and with BS, regardless of *U* presence (Table 2).

At D–14, regardless of *U*, [NO_3^-] was similar in all treatments (Fig. 3b). At D0 too [NO_3^-] was similar across treatments, but values were lower with *U*. At D+14, without *U*, PG, and PG-BA2 had significantly higher values than all other treatments, including those with *U* (Fig. 3b). Only PG-BA2 had different concentrations at different times, where they increased (Fig. 3b). At D0 and D+14, adding *U* resulted in significantly lower [NO_3^-] (Table 2). At D+14, without *U*, the 2 % application rate determined higher [NO_3^-] (Table 2). In treatments without *U* at D +14, BA determined significantly higher [NO_3^-], a finding seen at all sampling times with *U* (Table 2).

At D −14, the lowest [SO_4^{2-}] without *U* was observed in PG, PG-BA2, PG-BA5, and PG-BS2. With *U*, concentrations were higher, but no differences were measured (Fig. 3c). At D0, without *U*, PG-BS5 had the highest value, comparable to treatments with *U*. Without *U*, at D +14, PG-BA5 and PG-BS5 had the highest values. With *U*, PG-*U*-BS2 had the highest value (Fig. 3c). A significant [SO_4^{2-}] increase was measured in PG-BA5 and PG-BS5 (Fig. 3c). At D −14 and D0, *U* addition determined higher [SO_4^{2-}] (Table 2). At all sampling times, without *U*, [SO_4^{2-}] was higher with a 5 % biochar application and with BS (Table 2). Generally, [Cl^-], [NO_3^-], and [SO_4^{2-}] increased in control pots and those with biochar alone, while levels in *U* treatments decreased, though few cases were significant (Fig. 3). [F^-] and [NO_2^-] were found only at D-14 in *U* treatments (Suppl. Data Fig. 1).

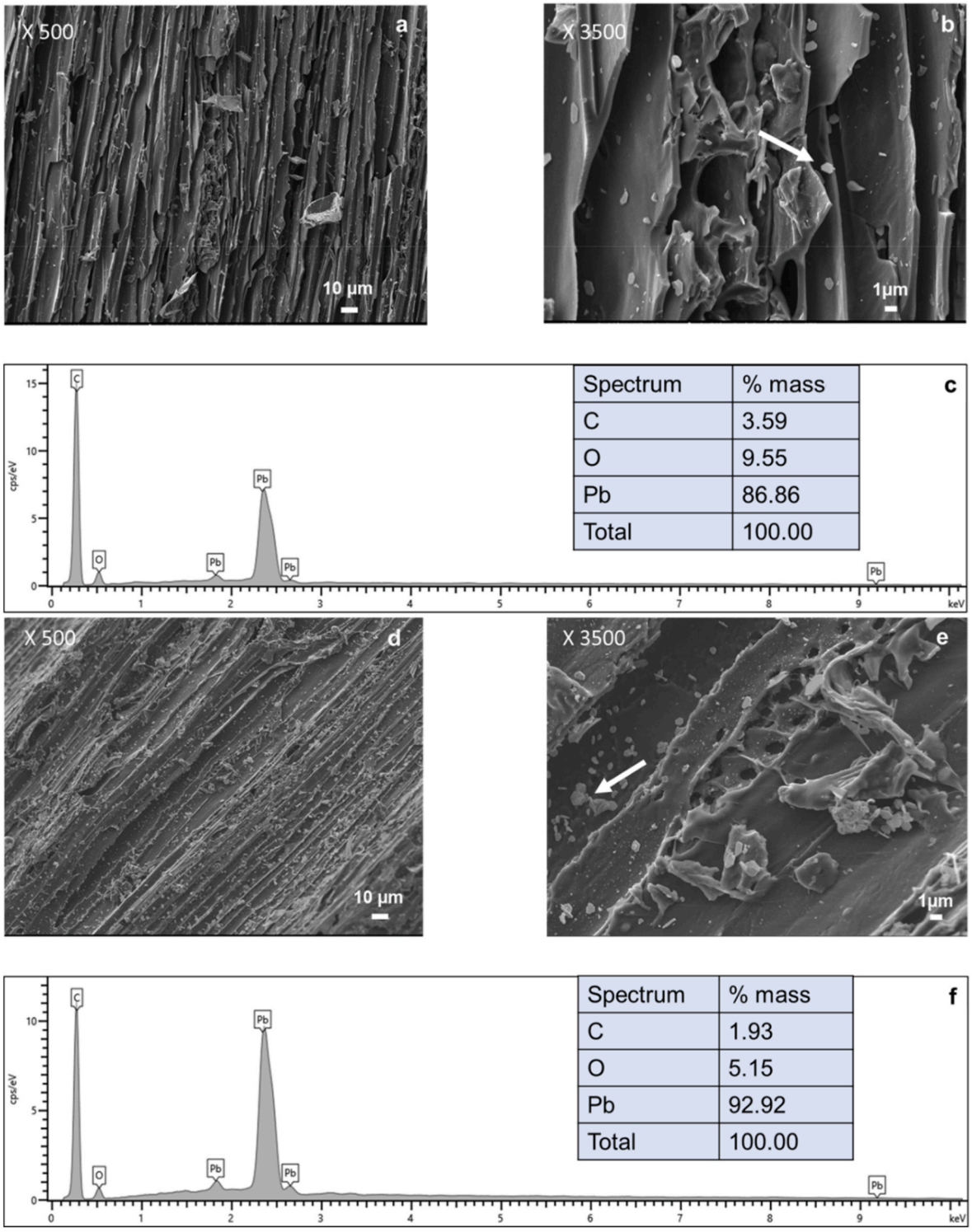

Fig. 1. SEM images and EDS spectra of *A. altissima* (a, b, c) and *S. gigantea* (d, e, f) derived biochar. The arrow on subplots b and e indicate the structure from which the EDS spectrum (c, f) was obtained. The table in the EDS spectrum indicated the % in mass of the identified elements.

Without *U*, As was measured only in PG-BS5 at D0 and D +14 (Fig. 3d). With *U*, As was measured from D-14, with no differences between treatments (Fig. 3d). At D0, [As] increased significantly, but at D +14, As decreased with no statistical differences between treatments. Without *U*, only PG-BS5 showed an increase from D0 and D +14. In treatments with *U*, As significantly increased from D-14 to D0, then significantly decreased from D0 to D+14 in PG-*U*, PG-*U*-BA2, and PG-*U*-BS5 (Fig. 3d). At all sampling times, *U* determined an increase in As (Table 2). Without *U*, a dose effect was quantified at D0: the 5 % biochar application determined higher [As]. Without *U*, the biochar type effect was significant at D0 with BS. With *U*, the biochar type effect was significant at D–14, where As was higher with BA, while at D0, As was higher with BS (Table 2).

Four cations were identified: sodium (Na^+), potassium (K^+), magnesium (Mg^{2+}), and calcium (Ca^{2+}), along with the toxic cationic metal, lead (Pb). At D −14, without *U*, there were no differences between

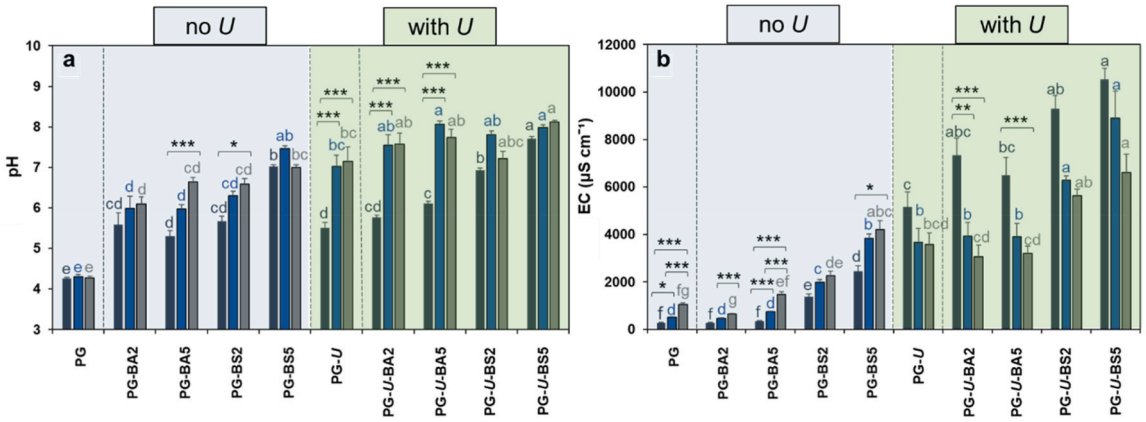

Fig. 2. Data represents the mean ± standard error of four replicates (n = 4) of soil pore water (SPW) pH (a), electric conductivity (EC; b), at the moment of soil mixtures preparation (D-14, represented by black bars and letters), seed sewing and the end of the two-week maturation period (D0, represented by blue bars and letters) and at the end of the two-week growth period (D+14, represented by grey bars and letters). The blue part of the figure represents treatments where no powdered *U. dioica* was applied; the green part represents treatments where it was added. Letters correspond to post-hoc comparisons at $p < 0.05$ between treatments within a specific sampling time. Asterisks represent significant post-hoc comparisons of the differences between SPW properties of the same treatment at different times: $p < 0.05$ (*), $p < 0.01$ (**), $p < 0.001$ (***). Legend of treatments in the list of abbreviations.

treatments in [Na^+]; lower values occurred with *U*, without differences between them (Fig. 4a). The same pattern was observed at D0 (Fig. 4a). At D+14, treatments without *U* PG had the highest value. With *U*, as in D −14 and D0, no differences emerged between treatments, with [Na^+] increasing throughout the experiment (Fig. 4a). At all sampling times, [Na^+] was significantly higher without *U* (Table 2). With *U*, a dose effect was quantified at D +14, with 2 % biochar application determining higher values (Table 2). A biochar type effect was measured at D0, without *U*, where BS determined higher values (Table 2).

At D-14, without *U*, the highest [K^+] were in PG-BS2 and PG-BS5 Fig. 4b). With *U*, the highest values were in PG-*U*-BS5 despite being lower than those with BS only. Similar findings were observed in D0 and D+14. Only PG and PG-BA5 showed different concentrations at different times, showing an increase (Fig. 4b). A biochar type effect was measured at all sampling times, regardless of *U*, with [K^+] being higher with BS (Table 2).

At D–14, without *U*, PG-BS5 had the highest [Mg^{2+}]. With *U*, values increased, but no statistical differences were found between them (Fig. 4c). The same findings were observed at D0, regardless of *U* application. At D+14, similar findings were observed (Fig. 4c). Without *U*, [Mg^{2+}] increased in PG, PG-BA5, PG-BS2, and PG-BS5 (Fig. 4c). At D-14 and D0, *U* determined higher [Mg^{2+}] (Table 2). At all sampling times, without *U*, BS determined higher [Mg^{2+}] (Table 2). At D0 and D +14, with *U*, the same biochar type effect was quantified (Table 2).

In treatments without *U*, at D −14, PG-BS5 showed the highest [Ca^{2+}]. With *U*, values were higher, with no difference among them (Fig. 4d). At D0, without *U*, the highest [Ca^{2+}] was in PG-BS5, surpassing that of *U* treatments (Fig. 4d). At D+14, without *U*, the highest values were in PG-BS5 and PG-BA5; with *U*, the values decreased, and PG-*U*-BS5 had the lowest (Fig. 4d). [Ca^{2+}] increased in PG, PG-BA5, PG-BS2, and PG-BS5; it decreased in PG-*U*-BA2 and PG-*U*-BS5 (Fig. 4d). There was a significant *U* effect, where *U* determined higher concentrations at D-14 and D0; however, at D+14, [Ca^{2+}] was higher without *U* (Table 2). At D+14, without *U*, 5 % biochar determined higher [Ca^{2+}] (Table 2). At D0 and D +14, with *U*, the [Ca^{2+}] was higher at the 2 % biochar application rate (Table 2). Finally, without *U*, at D −14 and D0, BS determined higher [Ca^{2+}] (Table 2).

At D-14, treatments without *U* showed lower [Pb] than PG, being lowest in PG-BS5. Treatments with *U* had higher [Pb], with no statistical differences among them (Fig. 4e). At D0, without *U*, PG had the highest [Pb], while PG-BA2, PG-BA5, PG-BS2, and PG-BS5 had lower levels. With *U*, PG-*U* had the highest concentration. The lowest was that of PG-*U*-BA5 (Fig. 4e). At D +14, without *U*, the highest [Pb] was that of PG, decreasing in all other treatments with no statistical differences, even amongst those with *U* (Fig. 4e). [Pb] significantly decreased within all the *U* treatments throughout the experiment, as well as in some treatments without *U* (Fig. 4e). At all sampling times, a *U* effect on SPW [Pb] was quantified, increasing levels at D–14, but lowering them at D0 and D +14 (Table 2). Without *U*, a dose effect was quantified at D −14 and D +14, where the 5 % application reduced [Pb] (Table 2). At all sampling times, without *U*, BS showed lower values. With *U*, the biochar type effect was significant at D −14, with BS determining lower concentrations, and at D0, but with BA determining lower concentrations (Table 2).

3.4. Plant growth characteristics

PG had the smallest biomass across all treatments, with no statistical difference compared to the stem mass of PG-BA2 and root mass of PG-BA2, PG-BA5, and PG-BS2 (Fig. 5a and b). PG-BA5 and PG-BS5 showed the highest leaf and stem dry weight of treatments without *U*, statistically similar to most treatments with *U* (Fig. 5a). Among those, PG-*U*-BA5 showed the highest stem and leaf values. (Fig. 5a). Without *U*, PG-BS5 had the highest root dry weight, similar to treatments with *U*, where PG-*U*-BA5 showed the highest values (Fig. 5b). *U* addition significantly increased the dry weight of leaves, stems, and roots (Table 3). In all organs, regardless of *U*, the 5 % biochar application determined higher dry weight values (Table 3). BS determined higher root masses without *U*, while with *U*, BA determined higher masses in all organs (Table 3).

3.5. Root morphological traits

Without *U*, in the 0–2 mm diameter class, PG-BS5 and PG-BA5 had longer fine root lengths. With *U*, PG-*U*-BA2, and PG-*U*-BA5 had the highest values of all treatments (Fig. 6b). In this diameter class, *U* incorporation determined higher root lengths (Table 3), and so did the 5 % biochar application, regardless of *U* (Table 3). With *U*, a statistical biochar type effect was measured: BA determined higher lengths (Table 3). In treatments without *U*, within the 0–0.5 mm class, PG-BS5 and PG-BA5 have the greatest fine root length, and PG-BA2 had the lowest, similar to PG (Fig. 6a). With *U*, the fine roots were longer in PG-*U*-BA5, PG-*U*-BS2 had the lowest (Fig. 6a). In this diameter class, *U* addition determined higher root lengths (Table 3). Without *U*, the 5 % biochar application determined higher lengths (Table 3). With *U*, a biochar-type effect was quantified: BA yielded higher values (Table 3).

Table 2
Quantification of the effect of the different amendments to the multi-heavy metal contaminated soil on soil pore water (SPW) measured properties. The effect of the stinging nettle was measured comparing treatments with and without *U* powder. The dose effect was measured comparing treatments with 2 and 5 % biochar application rates, separating the treatments without and with *U*. The biochar type effect was measured comparing treatments with BA and BS biochars, separating the treatments without and with *U*. Asterisks represent post-hoc comparisons; $p < 0.05$ (*), $p < 0.01$ (**), $p < 0.001$ (***), and ns (non-significant).

	U. dioica effect (no*U* vs + *U*)			Biochar dose effect no *U* (2 % vs 5 %)			Biochar dose effect +*U* (2 % vs 5 %)			Biochar type effect no *U* (BA vs BS)			Biochar type effect +*U* (BA vs BS)		
	D-14	D0	D+14	D-14	D0	D+14	D-14	D0	D+14	D-14	D0	D+14	D-14	D0	D+14
pH	5.57 ± 0.21	6.01 ± 0.24	6.11 ± 0.23	5.62 ± 0.14	6.14 ± 0.16	6.34 ± 0.14	6.34 ± 0.22	6.67 ± 0.14	7.39 ± 0.16	5.44 ± 0.15	5.98 ± 0.15	6.36 ± 0.14	5.93 ± 0.07	7.80 ± 0.16	7.64 ± 0.16
	6.40 ± 0.19	7.68 ± 0.11	7.55 ± 0.12	6.16 ± 0.33	6.71 ± 0.28	6.81 ± 0.09 *	6.91 ± 0.30	8.02 ± 0.05	7.92 ± 0.12	6.34 ± 0.26	6.88 ± 0.23	6.79 ± 0.10	7.31 ± 0.15	7.90 ± 0.61	7.66 ± 0.18
	**	***	***	**ns**	**ns**		**ns**	*	*	*	**	*	***	**ns**	**ns**
EC	949.3 ± 202.1	1506.3 ± 298.3	1921.7 ± 299.2	826.2 ± 212.5	1227.1 ± 291.1	1452.4 ± 316.4	8313.6 ± 560.8	5108.2 ± 526.9	4345.8 ± 549.1	317.4 ± 14.3	602.2 ± 51.8	1056.5 ± 166.6	6913.6 ± 504.3	3913.3 ± 375.9	3128.9 ± 265.3
	7759.9 ± 509.9	5338.7 ± 537.6	4416.4 ± 384.5	1405.2 ± 410.5	2284.4 ± 591.6	2831.6 ± 548.7	8509.3 ± 867.4	6402.1 ± 1116.8	4906.9 ± 752.7	1913.9 ± 235.2	2909.3 ± 362.9	3227.5 ± 415.5	9909.2 ± 417.7	7597.0 ± 730.8	6123.9 ± 423.5
	***	***	***	**ns**	**ns**	*	**ns**	**ns**	**ns**	***	***	***	***	***	***
[As]	bdl	0.06 ± 0.03	0.18 ± 0.07	bdl	bdl	bdl	0.72 ± 0.06	3.49 ± 0.51	1.14 ± 0.30	bdl	bdl	bdl	0.77 ± 0.05	2.18 ± 0.5 4.07 ±	0.90 ± 0.14
	0.71 ± 0.03	3.16 ± 0.31	1.00 ± 0.16	bgl –	0.14 ± 0.06 *	0.35 ± 0.14 **ns**	0.65 ± 0.03	2.75 ± 0.53	0.82 ± 0.16	bdl –	0.14 ± 0.06 *	0.35 ± 0.14 **ns**	0.59 ± 0.02	0.28 **	1.07 ± 0.32
	***	***	***				**ns**	**n**	**ns**				**		**ns**
[Pb]	12.97 ± 2.50	10.83 ± 2.72	8.61 ± 2.56	11.92 ± 1.11	7.23 ± 1.92	5.02 ± 1.35 1.52 ± 0.26	93.50 ± 8.50	1.66 ± 0.23	0.35 ± 0.06	11.23 ± 1.08	8.51 ± 1.59	5.19 ± 1.29	105.09 ± 7.28	0.96 ± 0.26	0.51 ± 0.19
	86.28 ± 5.50	1.58 ± 0.22	0.46 ± 0.08	4.68 ± 1.52	3.40 ± 1.01 *		82.15 ± 9.81	1.07 ± 0.28	0.58 ± 0.18	5.37 ± 1.91	2.11 ± 0.55	1.35 ± 0.22	70.57 ± 6.27	1.76 ± 0.21	0.42 ± 0.06
	***	***	***	**	**ns**		**ns-**	**ns**	**ns**	*	***	**	**	*	**ns**
[Cl^-]	222.77 ± 54.78	316.52 ± 62.34	378.11 ± 67.81	208.68 ± 80.63	294.74 ± 81.47	329.45 ± 79.96	870.37 ± 103.8	566.57 ± 85.06	570.27 ± 86.20	53.46 ± 2.87	89.62 ± 4.09	96.62 ± 23.86	573.32 ± 52.77	359.80 ± 45.4	337.85 ± 40.4
	840.55 ± 98.60	622.25 ± 90.81	567.60 ± 64.44	317.60 ± 103.6	424.54 ± 125.8	450.63 ± 150.9	980.30 ± 182.2	787.67 ± 200.29	626.29 ± 134.1	472.22 ± 74.39	629.66 ± 53.21	683.45 ± 71.10	1277.3 ± 114.0	994.44 ± 141.4	858.71 ± 67.9
	***	**	*	**ns**	**ns**	**ns**	**ns**	**ns**	**ns**	***	***	***	***	***	***
[$NO3^-$]	14.76 ± 1.64	10.88 ± 1.55	42.89 ± 8.64	11.53 ± 1.22	8.35 ± 0.56	58.64 ± 16.33	11.64 ± 7.95	1.45 ± 1.03	3.74 ± 1.42	11.06 ± 0.84	8.02 ± 0.53	59.75 ± 16.15	21.28 ± 7.35	4.53 ± 1.97	5.61 ± 0.94
	12.43 ± 3.74	2.63 ± 1.16	3.90 ± 0.98	11.84 ± 0.85	7.35 ± 1.13	19.23 ± 4.63	14.50 ± 4.49	3.08 ± 2.02	1.87 ± 0.92	12.31 ± 1.18	7.68 ± 1.17	18.12 ± 3.78	4.86 ± 3.27	Bdl *	bdl ***
	ns	***	***	**ns**	**ns**	*	**ns**	**ns**	**ns**	**ns**	**ns**	**	*		
[SO_4^{2-}]	120.00 ± 27.09	319.99 ± 70.58	573.09 ± 102.4	76.15 ± 14.59	225.78 ± 55.23	365.30 ± 78.14	902.99 ± 98.44	788.40 ± 117.95	522.92 ± 82.83	61.76 ± 5.47	152.05 ± 26.93	479.91 ± 123.2	754.26 ± 56.71	615.86 ± 127.7	403.10 ± 81.7
	813.11 ± 58.01	746.40 ± 88.83	469.79 ± 54.60	210.08 ± 52.2	552.48 ± 127.7	1020.68 ± 117.3	815.08 ± 62.99	780.62 ± 181.20	463.14 ± 92.07	224.47 ± 47.90	626.21 ± 101.1	906.07 ± 149.6	964.44 ± 88.50	953.16 ± 149.4	582.96 ± 81.2
	***	***	**ns**	*	*	***	**ns**	**ns**	**ns**	**	***	*	**ns**	**ns**	**ns**
[Na^+]	14.69 ± 0.68	31.10 ± 1.91	77.81 ± 5.50	14.92 ± 1.10	29.85 ± 1.00	62.55 ± 4.06	3.85 ± 0.37	8.48 ± 0.60	14.87 ± 0.95	14.57 ± 1.21	29.43 ± 1.04	74.58 ± 9.60	3.82 ± 0.30	7.80 ± 0.72	12.24 ± 1.08
	3.79 ± 0.18	8.17 ± 0.36	13.24 ± 0.60	14.54 ± 1.26	33.21 ± 1.24	79.75 ± 9.61	3.57 ± 0.20	8.00 ± 0.59	11.26 ± 0.60	14.90 ± 1.15	33.63 ± 1.01	67.72 ± 5.90	3.60 ± 0.30	8.68 ± 0.40	13.90 ± 0.91
	***	***	***	**ns**	**ns**	**ns**	**ns**	**ns**	**	**ns**	*	**ns**	**ns**	**ns**	**ns**
[K^+]	225.72 ± 61.77	332.71 ± 89.22	337.61 ± 86.70	179.81 ± 60.77	256.91 ± 85.75	269.01 ± 88.75	258.73 ± 27.05	197.05 ± 27.22	163.64 ± 30.93	42.20 ± 6.42	76.64 ± 16.53	121.17 ± 30.46	202.05 ± 19.19	139.29 ± 16.70	98.55 ± 12.81
	260.52 ± 24.71	222.35 ± 31.18	173.70 ± 22.94	377.50 ± 124.09	571.39 ± 173.56	564.99 ± 166.91	302.81 ± 50.83	294.57 ± 65.36	213.66 ± 44.97	515.12 ± 76.59	751.65 ± 108.27	712.83 ± 126.73	359.50 ± 36.28	352.33 ± 46.61	278.76 ± 25.96
	ns	**ns**	**ns**	**ns**	**ns**	**ns**	**ns**	**ns**	**ns**	***	***	***	**	***	***
[Mg^{2+}]	1.70 ± 0.24	4.41 ± 1.14	8.57 ± 1.35	1.39 ± 0.15	2.77 ± 0.43	6.12 ± 1.10 12.37 ±	15.45 ± 1.65	14.86 ± 1.18	11.08 ± 1.16	0.96 ± 0.13	1.78 ± 0.37	5.39 ± 0.80	13.70 ± 1.77	11.71 ± 1.39	8.62 ± 0.93
	13.76 ± 0.90	14.08 ± 1.00	10.35 ± 0.65	2.19 ± 1.54	7.66 ± 2.45	2.76 **ns**	12.94 ± 1.18	14.27 ± 1.94	9.41 ± 0.85	2.63 ± 0.39	8.65 ± 2.10	13.10 ± 2.60	14.69 ± 1.17	17.42 ± 0.97	11.86 ± 0.81
	***	***	**ns**	**ns**	**ns**		**ns**	**ns**	**ns**	***	**	**	**ns**	**	*
[Ca^{2+}]	13.52 ± 1.78	30.87 ± 5.00	59.10 ± 6.38	13.45 ± 1.16	24.51 ± 2.64	39.85 ± 5.28	66.89 ± 7.56	53.11 ± 3.01	40.20 ± 1.67	10.93 ± 1.31	22.03 ± 2.28	54.45 ± 9.06	61.90 ± 8.03	43.92 ± 4.93	37.51 ± 3.31
	58.85 ± 4.02	46.53 ± 2.87	35.01 ± 2.63	13.39 ± 1.83	46.15 ± 9.83	86.00 ± 8.50	51.71 ± 4.10	38.84 ± 4.55	27.63 ± 5.23	15.91 ± 1.10	48.63 ± 9.02	71.39 ± 12.23	56.58 ± 4.92	48.02 ± 4.33	30.32 ± 5.17
	***	**	***	**ns**	**ns**	***	**ns**	*	*	*	*	**ns**	**ns**	**ns**	**ns**

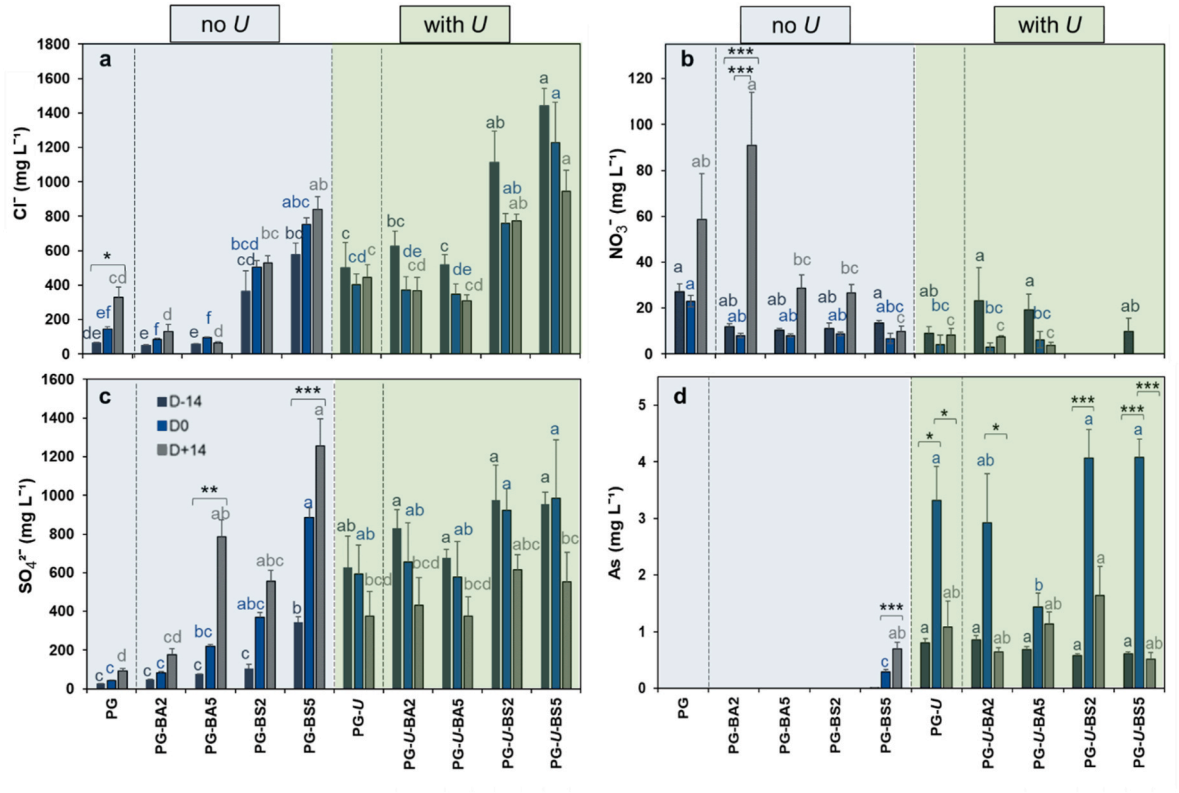

Fig. 3. Data represents the mean ± standard error of four replicates (n = 4) of soil pore water (SPW) anion (Chloride, a; Nitrate, b; Sulphate, c, and Arsenic, d) concentration at the moment of soil mixtures preparation (D-14, black bars and letters), seed sewing at the end of the two-week maturation period (D0, blue bars and letters) and at the end of the two-week growth period (D+14, grey bars and letters). The blue part of the figure represents treatments where no powdered *U. dioica* was applied; the green part represents treatments where it was added. Letters correspond to post-hoc comparisons at $p < 0.05$ between treatments within a specific sampling time. (. Asterisks represent significant post-hoc comparisons of the differences between SPW properties of the same treatment at different times: $p < 0.05$ (*), $p < 0.01$ (**), $p < 0.001$ (***). Legend of treatments in list of abbreviations.

Both in treatments with and without *U,* the 0.5–1 mm diameter class exhibited the same pattern as the previous class, with the same measured effects (Fig. 6a and Table 3). In the 1–2 mm diameter class, the highest fine root length was in PG-*U*-BA5, PG-*U*-BA2, and PG-BS5 (Fig. 6a). A *U* effect was calculated, where *U* determined higher lengths. With *U*, a biochar-type effect was measured, where BA determined higher values (Table 3). Statistical differences between the 0–0.5 and 1–2 mm classes were found; the highest length was in the 0–0.5 diameter class (Fig. 6a).

Without *U*, in the 0–2 mm diameter class, PG-BS5 had the highest biomass. With *U*, the greatest fine root biomass was in PG-*U*-BA2 and PG-*U*-BA5 (Fig. 6d). Biomass significantly increased with *U* (Table 3). Without *U*, the 5 % biochar application determined higher values (Table 3). A significant biochar-type effect was measured with *U*, where BA determined higher values (Table 3). In the 0–0.5 mm diameter class, without *U*, PG-BS5 and PG-BA5 had the highest root biomass, with *U*, PG-*U*-BA5, and PG-*U*-BA2 had the highest values (Fig. 6c). Samples with *U* have statistically higher biomasses (Table 3). Without *U*, the 5 % biochar application determined higher values (Table 3). With *U*, a significant biochar-type effect was measured, with BA showing higher values (Table 3). Similar findings were observed in the 0.5–1 mm class (Fig. 6c–Table 3). In the 1–2 mm class, no statistical differences were seen in samples without *U*. With *U*, the highest values were in PG-*U*-BA2 and PG-*U*-BA5 (Fig. 6c). In this diameter class, the same effects were measured as described above (Table 3). Finally, differences in biomass between the different classes were found, mainly showing an increase in the intermediate diameter class (Fig. 6c).

In the 0–2 mm diameter class, without *U*, PG-BS5 had the highest SRL. With *U*, PG-*U*-BA5 had the highest value, comparable to PG-BS5 (Fig. 6f). Regardless of *U*, the 5 % biochar application determined higher SRL values (Table 3). Without *U*, a biochar-type effect was measured, and BS determined higher SRLs. With *U*, the biochar-type effect was significant, too, but BA determined higher values (Table 3). In the 0–0.5 mm diameter class, without *U*, PG-BS5 had the highest values. With *U*, PG-*U*-BA5 had the highest SRL (Fig. 6e). A significant dose effect was measured without *U*, where the 5 % biochar application determined higher SRL values (Table 3). Without *U*, the use of BS determined higher values (Table 3). In the 0.5–1 mm diameter class, without *U*, PG-BS2 and PG-BS5 had the highest values. With *U*, PG-*U*-BA5 had the highest SRL (Fig. 6e). In this diameter class, regardless of *U*, the 5 % biochar application determined higher SRLs (Table 3). Without *U*, a biochar-type effect was quantified, and BS determined higher values (Table 3). In the 1–2 mm diameter class, without *U*, PG-BS2 had the highest values. With *U*, PG-*U*-BA5 had the highest values (Fig. 6e). In this diameter class, treatments without *U* had higher values (Table 3). A biochar-type effect was measured: without *U*, BS determined higher SRLs, and with *U*, BA determined higher values (Table 3).

3.6. Plant tissues As and Pb content

We found As only in roots (Fig. 7a–c). Without *U*, [As] was low, and PG's was below detection limit (b.d.l.), and PG-BS5 had the highest concentration (Fig. 7c). With *U*, the highest concentration was in PG-*U*, while PG-*U*-BA5 had the lowest (Fig. 7c). There was a significant *U* effect, where *U* increased [As] (Table 3). Without *U*, the 5 % biochar application determined higher values; with *U*, the 2 % biochar application rates determined higher values (Table 3).

Pb was found in aerial and belowground organs, with the highest values in PG (Fig. 7b–d). There were no differences in stem and leaf [Pb] in treatments without *U*. *U* significantly decreased the Pb content of

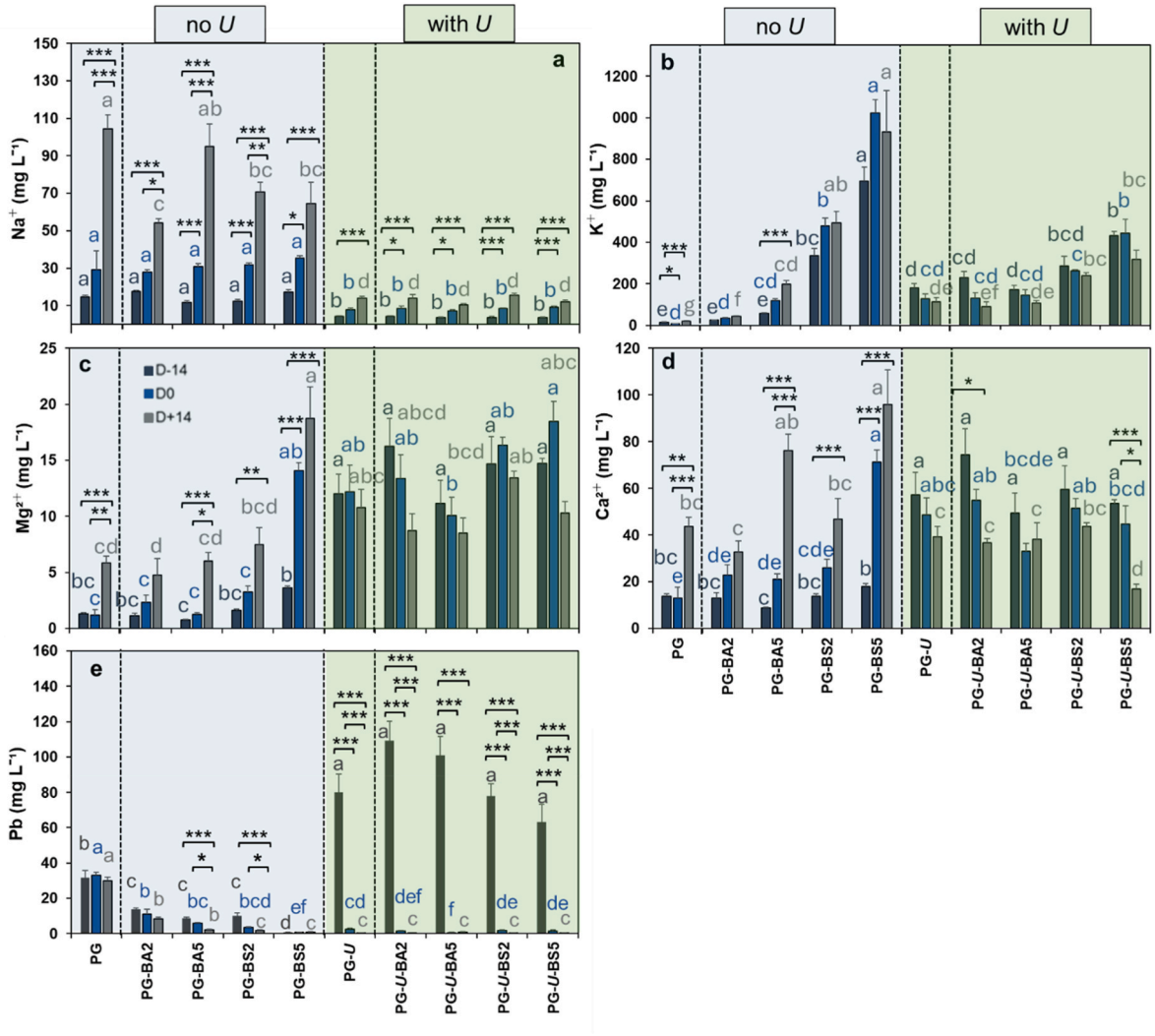

Fig. 4. Data represents the mean ± standard error of four replicates (n = 4) of soil pore water (SPW) cation (Sodium, a; Potassium, b; Magnesium, c; and Calcium, d, and Pb, e) concentration at the moment of soil mixtures preparation (D-14, black bars and letters), seed sewing at the end of the two-week maturation period (D0, blue bars and letters) and at the end of the two-week growth period (D+14, grey bars and letters). The blue part of the figure represents treatments where no powdered *U. dioica* was applied; the green part represents treatments where it was added. Letters correspond to mean values and post-hoc comparisons at $p < 0.05$ between treatments within a specific sampling time. Asterisks represent significant post-hoc comparisons of the differences between SPW properties of the same treatment at different times: $p < 0.05$ (*), $p < 0.01$ (**), $p < 0.001$ (***). Legend of treatments in list of abbreviations.

leaves and stems, with no differences between these treatments (Fig. 7b). There was a significant *U* effect in leaf [Pb], where *U* determined lower values (Table 3). The same effect was measured in stems (Table 3). Without *U*, a dose effect was measured in stem [Pb]: the 5 % biochar application determined lower values (Table 3). Without *U,* a biochar-type effect was measured in stem [Pb], where BS determined lower values (Table 3). Without *U*, PG had the highest root [Pb], while PG-BS5 had the lowest, with *U*, PG-*U*-BA5 had the lowest value (Fig. 7d). In root [Pb], regardless of *U*, a dose effect was quantified, where the 5 % biochar application determined lower values (Table 3). Without *U*, a biochar-type effect was quantified, where BS determined lower values (Table 3).

3.7. Soil enzymatic activity (GMEA)

The results of each enzymatic activity are shown in Supplementary data Fig. 2. The lowest recorded GMEA was in PG. Without *U*, no statistical differences existed between the treatments and PG. With *U*, the GMEA values were higher, peaking in PG-*U*-BA5 (Fig. 8). A significant *U* effect was measured, where *U* determined significantly higher values (Table 3). In addition, with *U*, GMEA had statistically higher values with the 5 % biochar application (Table 3).

4. Discussion

This study found that adding biochar from the pyrolysis of the biomass of the invasive *Ailanthus altissima* (BA) and *Solidago gigantea* (BS), coupled with *Urtica dioica* (*U*) powder, improved the physico-chemical characteristics of technosol. Our analysis highlighted that both pH and EC of the soil pore water (SPW) were higher than the control in all treatments, consistent with Nandillon et al. (2019b). The pH increased right after biochar was incorporated into the technosol (D-14), likely due to biochar's alkaline properties (Chintala et al., 2013). EC increased at the D-14, especially when BS and *U* powder were added, as previously tested using an aqueous stinging nettle extract (Maričić et al., 2021). These findings highlight the importance of the amendments' specific properties. EC tends to increase throughout the experiment in control and biochar-alone treatments, probably due to the gradual release of anions, cations, and inorganic carbonates from the technosol and biochar (Chintala et al., 2013). Interestingly, with *U*, EC, anions,

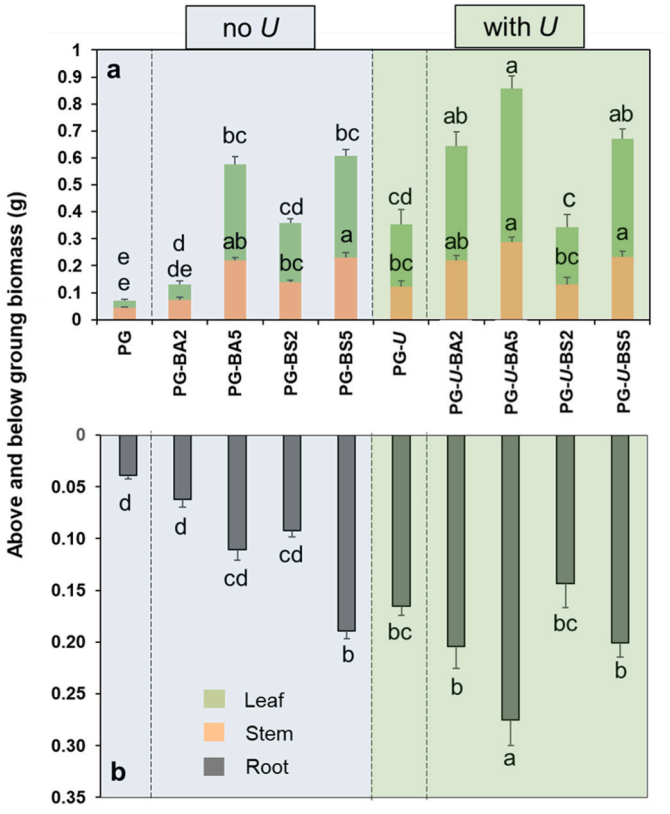

Fig. 5. Mean ± standard error of five replicates (n = 5) of *P. vulgaris* above (a) and belowground (b) biomass between the different treatments. The grey bar represents root mass, the brown bar represents stem mass, and the green bar represents leaf mass. The blue part of the figure represents treatments where no powdered *U. dioica* was applied; the green part represents treatments where it was added. Letters indicate post-hoc comparisons at $p < 0.05$. Legend of treatments in list of abbreviations.

and cations tended to decrease compared to the high initial values. This trend could derive from (*i*) a rapid release rate of charged particles by *U* powder addition to the technosol-biochar mix and (*ii*) the cations binding to the biochar. The binding of cations to biochar causes a lowering of EC in SPW and increases pH (Murtaza et al., 2011), explaining the high pH measured at the experiment's end for treatments containing *U*. Finally, the addition of *U* powder produced a similar pH and EC pattern to that observed with *Trifolium* dry leaves mixed with biochar in the same technosol (i.e., Pontgibaud; Lebrun et al., 2023).

The two types of biochar (alone or with *U*) determined different effects on the metal(loids) in SPW. Lebrun et al. (2022) reported that As' mobility increases when biochar is added to the technosol since As is present as an oxyanion. Indeed, pH increases with biochar incorporation, leading to more OH^- groups competing in the binding with Fe^{2+}, increasing the mobility of negatively charged As oxyanions, which might be bound to it (Beesley & Marmiroli 2011). Here, except in PG-BS5, As was not measured in SPW where biochar was added alone, likely due to the slightly acidic pH. Interestingly, we observed an increase in As when *U* was added to the biochar-technosol mix. This finding, exclusive to *U* treatments, might be explained by the pH increase and the anions' release in SPW (e.g., Cl^- and SO_4^{2-}, Table 2), which may compete with the As oxyanions, increasing their mobility. As increase with *U* addition could also be due to higher dissolved organic carbon (DOC) deriving from the *U* degradation, which competes with As for sorption sites in iron oxides (Nandillon et al., 2019 a). This was not observed when biochar was added alone, probably due to its stable carbon structure, which didn't cause DOC variation in SPW (Nandillon et al., 2019a). When As was measured in SPW at D+14, concentrations

Table 3
Quantification of the effect of the different amendments to the multi-heavy metal contaminated soil on plant growth, root morphological traits, metal uptake, and geometric enzymatic mean. The effect of the stinging nettle was measured comparing treatments with and without *U* powder. The dose effect was measured comparing treatments with 2 and 5 % biochar application rates, separating the treatments without and with U. The biochar type effect was measured comparing treatments with BA and BS biochars, separating the treatments without and with *U*. Asterisks represent post-hoc comparisons; $p < 0.05$ (*), $p < 0.01$ (**), $p < 0.001$ (***), and ns (non-significant).

	U. dioica effect (no*U* vs + *U*)	Biochar dose effect no *U* (2 % vs 5 %)	Biochar dose effect +*U* (2 % vs 5 %)	Biochar type effect no *U* (BA vs BS)	Biochar type effect +*U* (BA vs BS)
Leaf DW	0.21 ± 0.03 0.39 ± 0.03 ***	0.15 ± 0.03 0.37 ± 0.02 ***	0.34 ± 0.05 0.50 ± 0.03 **	0.21 ± 0.05 0.30 ± 0.03 **ns**	0.48 ± 0.04 0.34 ± 0.04 *
Stem DW	0.14 ± 0.01 0.21 ± 0.01 **	0.11 ± 0.01 0.22 ± 0.01 ***	0.18 ± 0.02 0.26 ± 0.01 **	0.14 ± 0.02 0.18 ± 0.02 **ns**	0.25 ± 0.02 0.18 ± 0.02 *
Root DW	0.10 ± 0.01 0.20 ± 0.01 ***	0.08 ± 0.01 0.15 ± 0.01 ***	0.18 ± 0.02 0.24 ± 0.02 *	0.09 ± 0.01 0.14 ± 0.01 *	0.24 ± 0.02 0.17 ± 0.01 *
Fine root length (0–0.5 mm)	93.76 ± 24.68 259.21 ± 63.33 **	27.54 ± 7.21 204.07 ± 34.08 ***	177.57 ± 55.36 441.03 ± 124.74 **ns**	68.73 ± 26.62 162.88 ± 45.80 **ns**	503.08 ± 109.72 115.52 ± 28.53 ***
Fine root length (0.5–1 mm)	76.38 ± 17.93 121.23 ± 82.85 *	36.35 ± 6.52 149.49 ± 12.67 ***	92.54 ± 14.07 180.76 ± 35.02 *	76.05 ± 21.52 109.78 ± 23.94 **ns**	190.87 ± 32.25 82.43 ± 9.99 **
Fine root length (1–2 mm)	5.94 ± 1.19 15.15 ± 2.60 ***	4.36 ± 0.68 9.43 ± 2.47 **ns**	14.54 ± 3.62 18.54 ± 5.19 **ns**	4.52 ± 0.55 9.26 ± 2.54 **ns**	26.08 ± 3.71 7.00 ± 1.19 ***
Fine root length (0–2 mm)	176.09 ± 39.95 395.59 ± 83.03 **	68.25 ± 12.37 362.99 ± 47.23 ***	284.66 ± 68.65 640.33 ± 162.94 *	149.32 ± 47.74 281.03 ± 71.09 **ns**	720.04 ± 141.07 204.94 ± 38.01 ***
Fine root biomass (0–0.5 mm)	0.004 ± 0.01 0.01 ± 0.002 **	0.002 ± 0.0003 0.009 ± 0.001 ***	0.012 ± 0.004 0.02 ± 0.004 **ns**	0.004 ± 0.001 0.007 ± 0.002 **ns**	0.02 ± 0.003 0.008 ± 0.002 ***
Fine root biomass (0.5–1 mm)	0.014 ± 0.002 0.03 ± 0.003 **	0.008 ± 0.0009 0.024 ± 0.001 ***	0.024 ± 0.004 0.036 ± 0.006 **ns**	0.015 ± 0.003 0.02 ± 0.003 **ns**	0.04 ± 0.005 0.019 ± 0.002 ***
Fine root biomass (1–2 mm)	0.004 ± 0.0005 0.014 ± 0.002 ***	0.003 ± 0.0005 0.005 ± 0.001 *	0.014 ± 0.003 0.016 ± 0.004 **ns**	0.004 ± 0.0005 0.004 ± 0.001 **ns**	0.02 ± 0.003 0.008 ± 0.001 **
Fine root biomass (0–2 mm)	0.02 ± 0.003 0.05 ± 0.007 ***	0.01 ± 0.001 0.04 ± 0.003 ***	0.05 ± 0.01 0.07 ± 0.01 **ns**	0.02 ± 0.004 0.03 ± 0.006 **ns**	0.09 ± 0.009 0.03 ± 0.005 ***
Fine root SRL (0–0.5 mm)	174.89 ± 11.59 179.70 ± 11.18 **ns**	136.40 ± 14.72 209.18 ± 10.70 **	177.80 ± 14.72 196.59 ± 22.95 **ns**	141.31 ± 16.13 204.27 ± 12.89 **	198.39 ± 22.61 176.00 ± 14.83 **ns**

(*continued on next page*)

Table 3 (*continued*)

	U. dioica effect (no*U* vs + *U*)	Biochar dose effect no *U* (2 % vs 5 %)	Biochar dose effect +*U* (2 % vs 5 %)	Biochar type effect no *U* (BA vs BS)	Biochar type effect +*U* (BA vs BS)
Fine root SRL (0.5–1 mm)	47.32 ± 3.85 44.61 ± 1.26 **ns**	43.86 ± 5.97 61.16 ± 2.04 *	39.55 ± 0.82 49.19 ± 1.32 ***	42.57 ± 5.50 62.45 ± 1.65 **	45.21 ± 2.76 43.53 ± 1.11 **ns**
Fine root SRL (1–2 mm)	18.14 ± 1.55 10.51 ± 0.33 ***	18.63 ± 2.39 22.61 ± 0.71 **ns**	10.16 ± 0.39 10.88 ± 0.72 **ns**	18.12 ± 2.17 23.12 ± 0.92 *	11.85 ± 0.40 9.19 ± 0.21 ***
Fine root SRL (0–2 mm)	64.01 ± 7.49 64.89 ± 4.85 **ns**	55.04 ± 10.15 92.88 ± 5.41 **	55.63 ± 4.12 81.41 ± 7.79 *	56.09 ± 9.94 91.84 ± 6.66 **	79.24 ± 8.93 57.81 ± 3.55 *
Root [As]	32.41 ± 8.31 570.09 ± 63.53 ***	8.81 ± 4.60 70.74 ± 13.03 ***	649.92 ± 54.67 303.16 ± 39.53 ***	26.25 ± 7.13 51.05 ± 16.09 **ns**	409.89 ± 66.27 533.48 ± 71.21 **ns**
Leaf [Pb]	159.33 ± 26.96 45.24 ± 5.14 ***	112.92 ± 15.86 87.21 ± 7.30 **ns**	42.27 ± 6.63 40.29 ± 8.45 **ns**	109.25 ± 17.73 92.42 ± 7.43 **ns**	33.60 ± 1.34 49.56 ± 10.70 **ns**
Stem [Pb]	337.74 ± 99.14 40.97 ± 2.86 ***	211.67 ± 19.96 147.91 ± 21.14 *	42.33 ± 4.52 34.50 ± 3.12 **ns**	218.99 ± 21.74 147.12 ± 18.39 *	36.79 ± 2.63 39.84 ± 5.15 **ns**
Root [Pb]	6321.50 ± 822.51 4812.31 ± 482.32 **ns**	5684.89 ± 461.00 3360.75 ± 333.05 ***	5973.53 ± 537.95 2657.96 ± 356.15 ***	5654.95 ± 509.68 3579.38 ± 373.46 **	3494.45 ± 548.60 5060.99 ± 725.21 **ns**
GMEA	0.035 ± 0.015 1.055 ± 0.18 ***	0.040 ± 0.021 0.045 ± 0.031 **ns**	0.67 ± 0.29 1.64 ± 0.16 *	0.064 ± 0.035 0.02 ± 0.01 **ns**	1.04 ± 0.36 1.26 ± 0.26 **ns**

were lower than those detected at D0 and similar to those measured when the growing media was prepared (D-14). The As reduction to the initial concentration could be due to (*i*) the entrapment of As on the biochar (Beesley and Marmiroli, 2011), (*ii*) the formation of spherical compounds between the arsenate anions and the biochar calcite (Yin et al., 2016), and (*iii*) plant uptake (Beesley et al., 2013). However, from SEM images, As was not observed on the biochar surface as the batch adsorption experiment did not account for a possible long-term effect. We also detected As in *P. vulgaris* roots partially explaining its reduction.

Pb was detected in SPW across all treatments, with the highest concentrations in treatments with *U* at D-14. Similar findings were obtained by Lebrun et al. (2023) with green manure addition. This finding could be related to higher concentrations of Ca^{2+}, Mg^{2+}, and K^{+}, which may displace H^{+} and Pb^{2+} from exchange sites of the technosol, increasing their concentrations (Murtaza et al., 2011). From D-14 onward, [Pb] in SPW decreased with the addition of biochar, which increases the pH, reducing cation metal mobility (Lebrun et al., 2022; Kumpiene et al., 2019). As reported by Wu et al. (2024), the higher pH may increase the negative surface charges of the biochar and technosol, causing the electrostatic adsorption of Pb. Moreover, our results highlighted Pb immobilization on the biochar surface through the formation of $PbCO_3$, resulting from the pre-existing carbonate phases in the biochar (Chafik et al., 2024; Rees et al., 2017). Previous findings showed that Pb absorption in aqueous solutions from woody species-derived biochar was higher than that of herbaceous ones (Ceriani et al., 2024). Here, our findings contradict our first hypothesis: we found that [Pb] in SPW was higher in pots treated with BA than those with BS, especially in the absence of *U,* as put in evidence in Table 2 (biochar type effect columns), highlighting that soil matrix strongly affects biochar's metal remediation efficiency. In the previous batch adsorption experiment, where the biochar was only in contact with the water (Ceriani et al., 2024), the higher surface area of woody species-derived biochar might have led to enhanced Pb stabilization. Here, the technosol's particles might have reduced the surface area effect by obstructing Pb contact with the biochar. This unexpected result, where BS alone immobilizes more than BA applied alone, might be due to its higher pH, as highlighted in Table 1, where BS' high alkalinity determines higher pH in SPW (Table 2), reducing the cationic metal's mobility. The higher pH of BS can be related to the biochar's composition. Specifically, it has been found that the higher ash contents of biochars determine higher pH values, and herbaceous species-derived biochars have been characterized to have higher ash contents and, consequently, pHs (Weber & Quicker 2018; Ceriani et al., 2024). The higher pH of BS also explains why the treatment PG-BS5 was the only one amongst the treatments with no *U* where As was detectable. Also, applying BS, with and without *U,* improved important SPW parameters for plant development, namely, pH, EC, $[SO_4^{2-}]$, $[K^{+}]$, $[Mg^{2+}]$, and $[Ca^{2+}]$, as highlighted in Table 2 (biochar type effect columns). This supports our second hypothesis and confirms that biochar from invasive herbaceous plants can benefit soil amendment (Ceriani et al., 2024). Furthermore, we can partially confirm our third hypothesis where adding *U* further improved the SPW properties and the positive effects of the two biochar types, increasing pH, EC, $[K^{+}]$, and $[Mg^{2+}]$ (at higher magnitudes in the case of BS), despite there being an increase in As in SPW *U*. Moreover, *U* addition, especially when added with BA, enhanced the Pb adsorption at D0 and D +14 (Table 2), suggesting a singular synergism between these two amendments.

Soil enzymatic activities respond to alterations in the edaphic environment, and are indicators of soil quality (Paz-Ferreiro et al., 2012) and bacterial communities' activity status (LeBrun et al., 2021). All six activities were higher in *U* treatments, suggesting this mixture of soil amendments effectively improves plant growth and potential phytoremediation in technosols (see also Nandillon et al. 2019a). In contrast to the improved soil enzymatic activities with biochar found by Arif et al. (2018), our results are in line with Lebrun et al. (2021) and Tang et al. (2020), where biochar reduces them. This reduction could be related to biochar's adsorption of organic and inorganic molecules, which inhibit certain enzymes' activity by blocking reaction sites (Elzobair et al., 2016). Still, applying biochar alone diminished the pseudo-total concentration of Pb in technosol and plants. However, given the polluted and impoverished technosol, adding *U* ameliorated soil properties and microbial activity and reduced Pb contamination, translating to healthier *P. vulgaris* plants, supporting our third hypothesis (see Table 3, *U* effect column). Organic matter derived from green manures, such as *U*, likely enhances microbial activity (Stefanowicz et al., 2020). This could explain the increase in βG, an enzyme that cleaves cellulose in glucose (de Mora et al., 2004), with *U* powder, as it is a more degradable form of organic matter than biochar. These findings support the notion that adding green manure or agronomic practices to increase soil nutrients can enhance local bacterial communities in degraded soils (Dalle Fratte et al., 2022).

Our phytoremediation study revealed that both biochar types, with or without *U*, improved the growth of *P. vulgaris*, confirming that the application of organic amendments reduces soil toxicity and enhances plant development (Kumar et al., 2020). Without *U* powder, no differences were detected between the two biochar types in the above-ground biomass. In contrast, *U* addition yielded differences between the two biochar types: plants grown with BA had a higher aboveground biomass than those with BS, supporting the third hypothesis, where *U* was hypothesized to improve the biochar's effects (Table 3). These differences could be related to the lower concentrations in SPW of Pb at D0 (Fig. 4e).

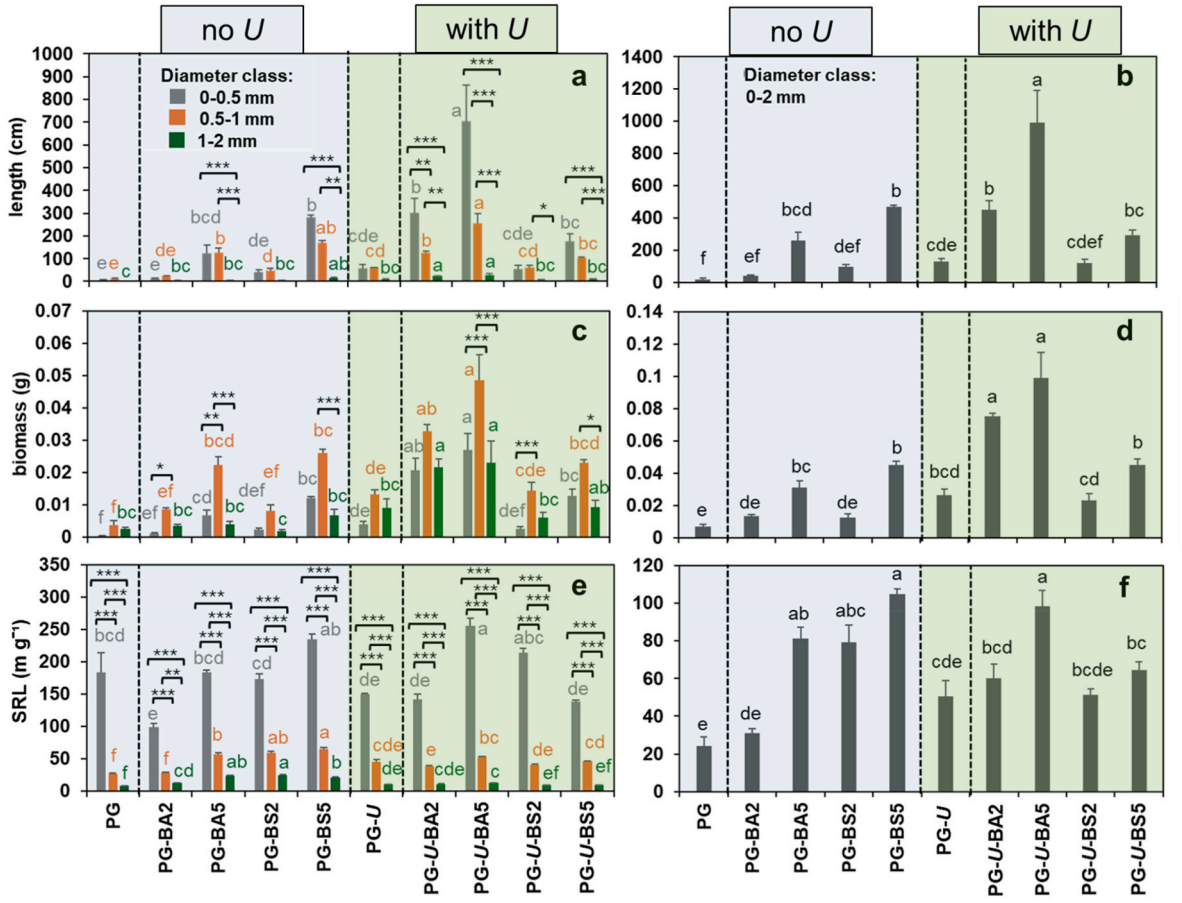

Fig. 6. Mean ± standard error of four replicates (n = 4) of *P. vulgaris*' fine root length (a, b), biomass (c, d) and SRL (e, f) in the different treatments. Panels b, d, and f represent the values in the 0–2 mm diameter class, while panels a, c, and e represent the values divided into different fine root diameter classes: 0–0.5 (grey bars and letters), 0.5–1 (orange bars and letters), 1–2 mm (green bars and letters). The blue part of the figure represents treatments where no powdered *U. dioica* was applied; the green part represents treatments where it was added. Letters correspond to post-hoc comparisons at $p < 0.05$ between treatments of a specific root diameter class. Asterisks represent significant post-hoc comparisons of the differences between fine root traits of the same treatment at different diameter classes: $p < 0.05$ (*), $p < 0.01$ (**), $p < 0.001$ (***). Legend of treatments in list of abbreviations.

The biochar application rate is important for aboveground plant development. The 5 % application, regardless of *U*, determined higher biomasses, likely related to improved soil conditions and reduced [Pb] in SPW.

Differences in root biomass emerged between the two biochar types depending on the *U* presence: higher root biomass was observed with BA and BS, respectively, with and without *U* addition (Fig. 5b). Considering the fine root fraction (0–2 mm diameter classes), the 5 % biochar application increased the length, biomass, and SRL compared to the control. The enhanced root development could be related to lower [Pb] and higher levels of macro/micronutrients (e.g., Cl^-, SO_4^{2-}, Mg^{2+}, K^+) in SPW (deriving from *U* addition with the biochar types or from BS when it was added alone), supporting the second and third parts of our hypothesis (as highlighted in Tables 2 and 3). Analyzing fine roots by diameter subclasses revealed that very fine fibrous roots (0–0.5 mm) were longer and had higher biomasses in plants treated with the 5 % biochar application and with *U*. Our data highlighted that root development in amended multi-heavy metal contaminated technosol is modulated by producing longer and more numerous fibrous roots, enhancing plant water and nutrient uptake (Polverigiani et al., 2011). Thicker fine roots showed significantly greater length, biomass, and specific root length (SRL) than the control for the 0.5–1 mm diameter class. Only SRL was significantly higher in the 1–2 mm diameter class than PG. Also, the length and biomass of this latter diameter class were significantly higher only with BA and *U* compared to PG. All fine root categories were more developed within this treatment (BA with *U*), suggesting that *U* can enhance the BA's effects despite its characteristics being suboptimal (e.g., total nutrient content) (Ceriani et al., 2024). The higher SRL of thicker fine roots compared to the control indicates a plastic strategy to increase the volume of soil exploited (Ostonen et al., 2007; Montagnoli et al., 2019). This response is likely due to the improved nutrient conditions and reduced metal stress brought by the biochar and *U*, enabling plants to invest in resource pre-emption. The increase in fine root functional traits from biochar application aligns with the findings of Simiele et al. (2022) in potted tomato plants, supporting our second (increased plant development with herbaceous IAPS-derived biochar, BS) and third hypotheses (improved soil conditions and plant growth with *U* and biochar types) (Table 3). It is important to note that biochar's impact on fine root traits varies with different soils and land use legacies, resulting in mixed outcomes. For example, biochar addition in vineyards reduced fine root length and biomass, probably because it improved water and nutrient availability, lessening the plant's investments toward resource pre-emption (Montagnoli et al., 2021; Baronti et al., 2022; Beatrice et al., 2024). Plants may afford to reduce foraging in optimal soil conditions, whereas here, root traits increase as there is an acidic and polluted soil as the plants need the resources to face the extreme soil conditions. Recent studies suggest that acquisitive root traits, such as high SRLs, may promote heavy-metal translocation (Wang et al., 2024), despite having observed that treatments with biochar alone had the highest overall SRL (0–2 mm) and had higher [Pb] in the aerial parts, we cannot fully confirm Wang's hypothesis, as biochar reduces the mobility of metals.

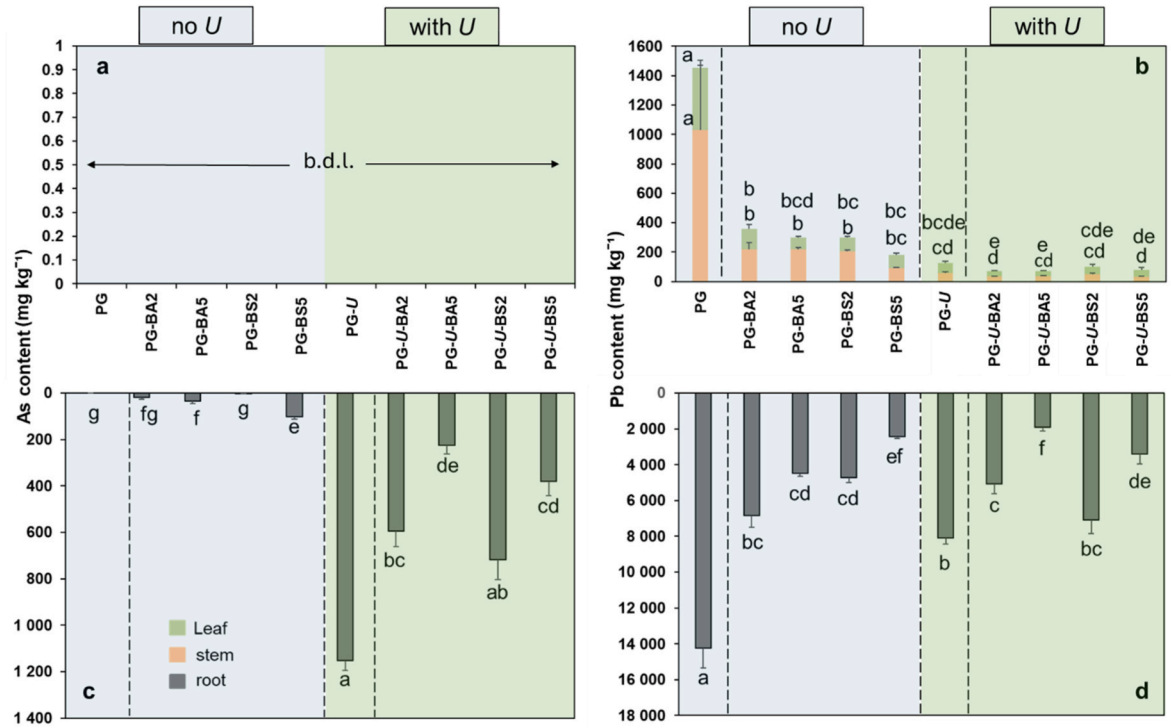

Fig. 7. Mean ± standard error of five replicates (n = 5) of Arsenic (As) (Fig. 4a–c) and Lead (Pb) concentration (Fig. 4b–d) in *P. vulgaris* organ (leaf, stem, root) between the different treatments. The blue part of the figure represents treatments where no powdered *U. dioica* was applied; the green part represents treatments where it was added. Letters indicate post-hoc comparisons at $p < 0.05$. Legend of treatments in list of abbreviations.

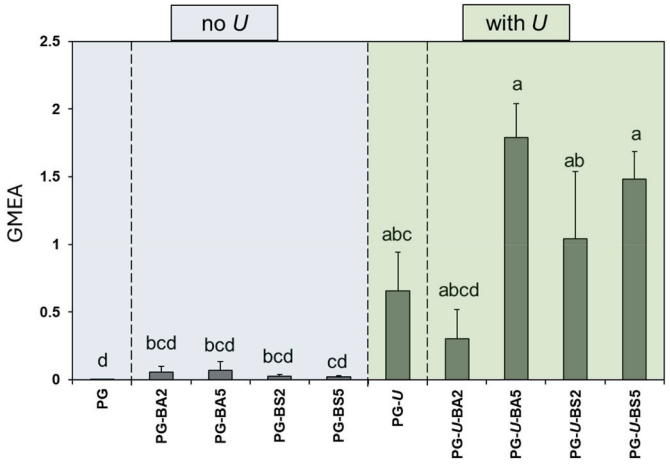

Fig. 8. Mean ± standard error of three replicates (n = 3) of the geometric mean enzymatic activities (GMEA). The blue part of the figure represents treatments where no powdered *U. dioica* was applied; the green part represents treatments where it was added. Letters indicate post-hoc comparisons at $p < 0.05$. Legend of treatments in list of abbreviations.

As was not present in the organs of *P. vulgaris* grown in unamended technosol (control), and it was detected only in the roots of plants grown with amendments, indicating a lack of translocation to shoots. When biochar was added alone to the technosol, [As] in the root tissues were low, while plants showed the highest [As] with *U* in the biochar-soil mix. These findings reflect those of As in SPW that were below detection limit (b.d.l.) in the control and biochar alone treatments but highest with *U*. Also, the increase in overall SRL (0–2 mm) observed in plants grown in the amended soil might have contributed to the As uptake in their roots. Contrary to As, Pb was found in the shoots, highlighting a translocation of Pb from roots to aboveground organs. The highest [Pb] was found in PG, particularly in roots, consistent with previous findings (Nandillon et al., 2019a). Interestingly, [Pb] in the root system was lower with the 5 % biochar application. This might be due to the higher pH, reducing Pb mobility, and the higher available surface for $PbCO_3$ precipitation (Rees et al., 2017). Plants grown with biochar and *U* had lower [Pb] than those with biochar only in their aboveground organs. This result supports previous findings (Bolan et al., 2014; Nandillon et al., 2019 b) suggesting that *U* powder also helps reduce Pb mobility and plant uptake. The additional organic material from *U* may help further entrap Pb, but our combination of amendments made As more available, especially with *U*. Despite this, the IAPS-derived biochar combined with a widespread weed (*U*) is a highly efficient and novel approach. It enhances phytoremediation using waste material, improving the system's efficiency by simultaneously addressing two environmental challenges, such as biological invasion and soil pollution. This approach, as demonstrated by Kochanek et al. (2022), not only proves profitable but also encourages a circular economy approach to environmental problems. Our results are also important within the United Nations Sustainable Development Goal (SDG) perspective (https://sdgs.un.org/goals). They align with goal number 15 (Life on Land), as this study offers a method to control IAPS and restore degraded ecosystems and polluted soils. The biochar and its combination with U effectively stabilized Pb and reduced its concentration in SPW, enhancing fine root development. The present study also aligns with goal 12 (Responsible Consumption and Production), focusing on converting waste biomasses into valuable resources. In addition, the proposed approach has the potential to be applied in many different sectors and, thus, aligns with other goals such as water pollution control (goal 6, Clean water and sanitation; He et al., 2022) and bioenergetic processes, e.g., anaerobic digestion (goal 7, Affordable and clean energy; Kochanek et al., 2022). Finally, few studies have focused on the specific combinations of IAPS-derived biochar with invasive widespread native weeds such as *U* in the context of multi-heavy-metal contamination. This highlights the originality of this work and its potential to provide new perspectives

towards IAPS management and a circular approach to phytoremediation (Wang et al., 2024b). It also provides novel insights into fine root response to an amended multi-heavy metal polluted soil.

5. Conclusion

Both biochars improved the technosol characteristics and plant growth. However, our findings contrasted the hypothesis that biochar from the invasive woody species *A. altissima* (BA) would more effectively stabilize Pb. The ameliorating effects were especially detected with the invasive herbaceous *S. gigantea* (BS) biochar. BS probably better stabilized Pb because of its higher pH, which helps reduce metal stress and promote plant growth. As we hypothesized, applying *U. dioica* powder (*U*) improved the technosol characteristics, enhancing the effects of the biochar alone. Interestingly, with *U* addition, BA became more effective in reducing Pb mobility. The combination of BA and *U* improved *P. vulgaris* seedlings' growth, leading to higher above- and below-ground biomasses and more developed fine root systems. *U* addition improved soil enzymatic activities, demonstrating its importance for the soil microbiome. Overall, adding biochar and *U*, independently of the biochar type, application rate, and combination, stimulated fine root development and a more efficient cost-to-benefit ratio (SRL), potentially contributing to metal(loids) uptake. Adding biochar and *U* to the technosol is a promising tool for stabilizing multi-heavy metal-contaminated soils and enhancing plant growth and phytoremediation efficiency. However, adding these amendments determined specific effects for each metal(loids). The addition of amendments diminished Pb-related toxicity but caused an increase in As mobility. This underscores the importance of assessing the soil, amendments, and toxic elements to establish effective *in-situ* phytoremediation. Our study enhances the understanding of sustainable soil management practices in the context of alien plant invasion.

CRediT authorship contribution statement

Alex Ceriani: Writing – original draft, Visualization, Investigation, Formal analysis, Data curation. **Yassine Chafik:** Visualization, Validation, Investigation, Formal analysis. **Alessio Miali:** Investigation, Formal analysis. **Sylvain Bourgerie:** Validation, Methodology, Investigation, Formal analysis. **Michele Dalle Fratte:** Writing – review & editing, Visualization, Validation. **Bruno E.L. Cerabolini:** Visualization, Validation, Resources. **Domenico Morabito:** Validation, Supervision, Resources, Project administration, Methodology, Conceptualization. **Antonio Montagnoli:** Writing – review & editing, Writing – original draft, Validation, Supervision, Resources, Project administration, Methodology, Conceptualization.

Declaration of generative AI and AI-assisted technologies in the writing process

During the preparation of this work, the author(s) used Grammarly in order to ameliorate the readability and language of the manuscript. After using this tool/service, the author(s) reviewed and edited the content as needed and take(s) full responsibility for the content of the publication.

Funding

Alex Ceriani was funded by the NOP PhD programs on green topics of the Italian Ministry of University and Research (MUR). Michele Dalle Fratte was funded by Fondazione Lombardia per l'Ambiente (FLA).

Declaration of competing interest

The authors declare that they have no known competing financial interests or personal relationships that could have appeared to influence the work reported in this paper.

Appendix A. Supplementary data

Supplementary data to this article can be found online at https://doi.org/10.1016/j.chemosphere.2025.144435.

Data availability

Data will be made available on request.

References

Arif, M.S., Riaz, M., Shahzad, S.M., Yasmeen, T., Ashraf, M., Siddique, M., Mubarik, M.S., Bragazza, L., Buttler, A., 2018. Fresh and composted industrial sludge restore soil functions in surface soil of degraded agricultural land. Sci. Total Environ. 619–620, 517–527. https://doi.org/10.1016/j.scitotenv.2017.11.143.

Baronti, S., Montagnoli, A., Beatrice, P., Danieli, A., Maienza, A., Vaccari, F.P., Casini, D., Di Gennaro, S.F., 2024. Above-and below-ground morpho-physiological traits indicate that biochar is a potential peat substitute for grapevine cuttings nursery production. Sci. Rep. 14 (17185). https://doi.org/10.1038/s41598-024-67766-4.

Baronti, S., Magno, R., Maienza, A., Montagnoli, A., Ungaro, F., Vaccari, F.P., 2022. Long term effect of biochar on soil plant water relation and fine roots: results after 10 years of vineyard experiment. Sci. Total Environ. 851. https://doi.org/10.1016/j.scitotenv.2022.158225.

Beatrice, P., Miali, A., Baronti, S., Chiatante, D., Montagnoli, A., 2023. Plant growth in LED-sourced biophilic environments is improved by the biochar amendment of low-fertility soil, the reflection of low-intensity light, and a continuous photoperiod. Plants 12 (18). https://doi.org/10.3390/plants12183319.

Beatrice, P., Dalle Fratte, M., Baronti, S., Miali, A., Genesio, L., Vaccari, F.P., Cerabolini, B.E.L., Montagnoli, A., 2024. The long-term effect of biochar application to Vitis vinifera L. reduces fibrous and pioneer root production and increases their turnover rate in the upper soil layers. Front. Plant Sci. 15. https://doi.org/10.3389/fpls.2024.1384065.

Beesley, L., Moreno-Jiménez, E., Gomez-Eyles, J.L., 2010. Effects of biochar and greenwaste compost amendments on mobility, bioavailability and toxicity of inorganic and organic contaminants in a multi-element polluted soil. Environ. Pollut. 158 (6), 2282–2287. https://doi.org/10.1016/j.envpol.2010.02.003.

Beesley, L., Marmiroli, M., 2011. The immobilisation and retention of soluble arsenic, cadmium and zinc by biochar. Environ. Pollut. 159 (2), 474–480. https://doi.org/10.1016/j.envpol.2010.10.016.

Beesley, L., Marmiroli, M., Pagano, L., Pigoni, V., Fellet, G., Fresno, T., Vamerali, T., Bandiera, M., Marmiroli, N., 2013. Biochar addition to an arsenic contaminated soil increases arsenic concentrations in the pore water but reduces uptake to tomato plants (*Solanum lycopersicum* L.). Sci. Total Environ. 454–455, 598–603. https://doi.org/10.1016/j.scitotenv.2013.02.047.

Biederman, L.A., Harpole, W.S., 2013. Biochar and its effects on plant productivity and nutrient cycling: a meta-analysis. Global Change Biology Bioenergy 5, 202–214.

Bolan, N., Kunhikrishnan, A., Thangarajan, R., Kumpiene, J., Park, J., Makino, T., Kirkham, M.B., Scheckel, K., 2014. Remediation of heavy metal(loid)s contaminated soils - to mobilize or to immobilize?. In: Journal of Hazardous Materials, vol. 266 Elsevier, pp. 141–166. https://doi.org/10.1016/j.jhazmat.2013.12.018.

Ceriani, A., Fratte, M.D., Agosto, G., Montagnoli, A., Enrico, B., Cerabolini, L., 2023. Using plant functional traits to define the biomass energy potential of invasive alien plant species. Plants 12 (3198). https://doi.org/10.3390/plants12183198.

Ceriani, A., Dalle Fratte, M., Agosto, G., Beatrice, P., Reguzzoni, M., Bettucci, L., Casini, D., Cerabolini, B.E.L., Montagnoli, A., 2024. Woody and herbaceous invasive alien plant species-derived biochars are potentially optimal for soil amendment, soil remediation, and carbon storage. GCB Bioenergy 16 (2). https://doi.org/10.1111/gcbb.13117.

Chafik, Y., Hassan, S.H., Lebrun, M., Sena-Velez, M., Cagnon, B., Carpin, S., Boukroute, A., Bourgerie, S., Morabito, D., 2024. Biochar characteristics and Pb2+/Zn2+ sorption capacities: the role of feedstock variation. Int. J. Environ. Sci. Technol. https://doi.org/10.1007/s13762-024-05646-0.

Chen, D., Liu, X., Bian, R., Cheng, K., Zhang, X., Zheng, J., Joseph, S., Crowley, D., Pan, G., Li, L., 2018. Effects of biochar on availability and plant uptake of heavy metals – a meta-analysis. J. Environ. Manag. 222, 76–85. https://doi.org/10.1016/j.jenvman.2018.05.004.

Chintala, R., Mollinedo, J., Schumacher, T.E., Malo, D.D., Julson, J.L., 2013. Effect of biochar on chemical properties of acidic soil. Arch. Agron Soil Sci. 60 (3), 393–404. https://doi.org/10.1080/03650340.2013.789870.

Cordero, I., Snell, H., Bardgett, R.D., 2019. High throughput method for measuring urease activity in soil. Soil Biol. Biochem. 134, 72–77. https://doi.org/10.1016/j.soilbio.2019.03.014.

Dalle Fratte, M., Montagnoli, A., Anelli, S., Armiraglio, S., Beatrice, P., Ceriani, A., Lipreri, E., Miali, A., Nastasio, P., Enrico, B., Cerabolini, L., 2022. Mulching in lowland hay meadows drives an adaptive convergence of above- and below-ground traits reducing plasticity and improving biomass: a possible tool for enhancing phytoremediation. Front. Plant Sci. 1–17. https://doi.org/10.3389/fpls.2022.1062911. November.

de Mendiburu, F., 2023. Agricolae: statistical procedures for agricultural research. R package version 1, 3–7. https://CRAN.R-project.org/package=agricolae.

de Mora, A. P. De, Ortega-Calvo, J.J., Cabrera, F., Madejón, E., 2004. Changes in enzyme activities and microbial biomass after "in situ" remediation of a heavy metal-contaminated soil. Appl. Soil Ecol. 28 (2), 125–137. https://doi.org/10.1016/j.apsoil.2004.07.006.

Elzobair, K.A., Stromberger, M.E., Ippolito, J.A., Lentz, R.D., 2016. Contrasting effects of biochar versus manure on soil microbial communities and enzyme activities in an aridisol. Chemosphere 142, 145–152. https://doi.org/10.1016/j.chemosphere.2015.06.044.

EU law, 2014. https://eur-lex.europa.eu/eli/reg/2014/1143/oj.

Feng, Q., Wang, B., Chen, M., Wu, P., Lee, X., Xing, Y., 2021. Invasive plants as potential sustainable feedstocks for biochar production and multiple applications: a review. Resour. Conserv. Recycl. 164 (June 2020), 105204. https://doi.org/10.1016/j.resconrec.2020.105204.

Fischer, D., Glaser, B., 2012. Synergisms between compost and biochar for sustainable soil amelioration. In: Management of Organic Waste. InTech.

Haubrock, P.J., Cuthbert, R.N., Sundermann, A., Diagne, C., Golivets, M., Courchamp, F., 2021. Economic costs of invasive species in Germany. NeoBiota 67, 225–246. https://doi.org/10.3897/neobiota.67.59502.

He, M., Xu, Z., Hou, D., Gao, B., Cao, X., Ok, Y.S., Rinklebe, J., Bolan, N.S., Tsang, D.C. W., 2022. Waste-derived biochar for water pollution control and sustainable development. Nat. Rev. Earth Environ. 3 (7), 444–460. https://doi.org/10.1038/s43017-022-00306-8. Springer Nature.

Ippolito, J.A., Cui, L., Kammann, C., Wrage-Mönnig, N., Estavillo, J.M., Fuertes-Mendizabal, T., Cayuela, M.L., Sigua, G., Novak, J., Spokas, K., Borchard, N., 2020. Feedstock choice, pyrolysis temperature and type influence biochar characteristics: a comprehensive meta-data analysis review. Biochar 2 (4), 421–438. https://doi.org/10.1007/s42773-020-00067-x.

Jia, W., Wang, B., Wang, C., Sun, H., 2017. Tourmaline and biochar for the remediation of acid soil polluted with heavy metals. J. Environ. Chem. Eng. 5 (3), 2107–2114. https://doi.org/10.1016/j.jece.2017.04.015.

Kochanek, J., Soo, R.M., Martinez, C., Dakuidreketi, A., Mudge, A.M., 2022. Biochar for intensification of plant-related industries to meet productivity, sustainability and economic goals: a review. In: Resources, Conservation and Recycling, vol. 179. Elsevier B.V. https://doi.org/10.1016/j.resconrec.2021.106109.

Kumar, A., Bhattacharya, T., Mozammil Hasnain, S.M., Kumar Nayak, A., Hasnain, M.S., 2020. Applications of biomass-derived materials for energy production, conversion, and storage. Materials Science for Energy Technologies 3, 905–920. https://doi.org/10.1016/j.mset.2020.10.012.

Kumpiene, J., Bert, V., Dimitriou, I., Eriksson, J., Friesl-Hanl, W., Galazka, R., Herzig, R., Janssen, J., Kidd, P., Mench, M., Müller, I., Neu, S., Oustriere, N., Puschenreiter, M., Renella, G., Roumier, P.H., Siebielec, G., Vangrosveld, J., Manier, N., 2014. Selecting chemical and ecotoxicological test batteries for risk assessment of trace element-contaminated soils (phyto) managed by gentle remediation options (GRO). Sci. Total Environ. 496, 510–522.

Kumpiene, J., Antelo, J., Brännvall, E., Carabante, I., Ek, K., Komárek, M., Söderberg, C., Wårell, L., 2019. In situ chemical stabilization of trace element-contaminated soil – field demonstrations and barriers to transition from laboratory to the field – a review. In: Applied Geochemistry, vol. 100. Elsevier Ltd, pp. 335–351. https://doi.org/10.1016/j.apgeochem.2018.12.003.

Lebrun, M., Miard, F., Van Poucke, R., Tack, F.M.G., Scippa, G.S., Bourgerie, S., Morabito, D., 2021. Effect of fertilization, carbon-based material, and redmud amendments on the bacterial activity and diversity of a metal(loid) contaminated mining soil. Land Degrad. Dev. 32 (8), 2618–2628. https://doi.org/10.1002/ldr.3929.

Lebrun, M., Miard, F., Trakal, L., Bourgerie, S., Morabito, D., 2022. Chemosphere the reduction of the As and Pb phytotoxicity of a former mine technosol depends on the amendment type and properties, 300(December 2021). https://doi.org/10.1016/j.chemosphere.2022.134592.

Lebrun, M., Palmeggiani, G., Renouard, S., Chafik, Y., Cagnon, B., Bourgerie, S., Morabito, D., 2023. Natural ageing of biochar improves its benefits to soil Pb immobilization and reduction in soil phytotoxicity. Environ. Geochem. Health 45 (8), 6109–6135. https://doi.org/10.1007/s10653-023-01617-5.

Maričíć, B., Radman, S., Romić, M., Perković, J., Major, N., Urlić, B., Palčić, I., Ban, D., Zorić, Z., Ban, S.G., 2021. Stinging nettle (Urtica dioica l.) as an aqueous plant-based extract fertilizer in green bean (Phaseolus vulgaris l.) sustainable agriculture. Sustainability 13 (7). https://doi.org/10.3390/su13074042.

Montagnoli, A., Dumroese, R.K., Terzaghi, M., Onelli, E., Scippa, G.S., Chiatante, D., 2019. Seasonality of fine root dynamics and activity of root and shoot vascular cambium in a Quercus ilex L. forest (italy). For. Ecol. Manag. 431, 26–34. https://doi.org/10.1016/j.foreco.2018.06.044.

Montagnoli, A., Baronti, S., Alberto, D., Chiatante, D., Scippa, G.S., Terzaghi, M., 2021. Pioneer and fibrous root seasonal dynamics of Vitis vinifera L. are affected by biochar application to a low fertility soil: a rhizobox approach. Sci. Total Environ. 751, 141455. https://doi.org/10.1016/j.scitotenv.2020.141455.

Murtaza, G., Haynes, R.J., Naidu, R., Belyaeva, O.N., Kim, K.R., Lamb, D.T., Bolan, N.S., 2011. Natural attenuation of Zn, Cu, Pb and Cd in three biosolids-amended soils of contrasting pH measured using rhizon pore water samplers. Water Air Soil Pollut. 221 (1–4), 351–363. https://doi.org/10.1007/s11270-011-0795-8.

Nandillon, R., Miard, F., Lebrun, M., Gaillard, M., Sabatier, S., Bourgerie, S., Battaglia-Brunet, F., Morabito, D., 2019a. A. Effect of biochar and amendments on Pb and As phytotoxicity and phytoavailability in a technosol. Clean 1–11. https://doi.org/10.1002/clen.201800220.

Nandillon, R., Lahwegue, O., Miard, F., Lebrun, M., Gaillard, M., Sabatier, S., Battaglia-Brunet, F., Morabito, D., Bourgerie, S., 2019b. B. Potential use of biochar, compost and iron grit associated with Trifolium repens to stabilize Pb and As on a multi-contaminated technosol. Ecotoxicol. Environ. Saf. 182 (July), 109432. https://doi.org/10.1016/j.ecoenv.2019.109432.

Ostonen, I., Püttsepp, Ü., Biel, C., Alberton, O., Bakker, M.R., Lõhmus, K., et al., 2007. Specific root length as an indicator of environmental change. Plant Biosyst. 141, 426–442. https://doi.org/10.1080/11263500701626069.

Parven, A., Meftaul, I.M., Venkateswarlu, K., Segovia, A.C., Megharaj, M., 2025. Potted garden pea grown in presence of pre-emergence herbicides: impacts on soil enzymes and human health. J. Food Compos. Anal. 138. https://doi.org/10.1016/j.jfca.2024.106985.

Paz-Ferreiro, J., Gascó, G., Gutiérrez, B., Méndez, A., 2012. Soil biochemical activities and the geometric mean of enzyme activities after application of sewage sludge and sewage sludge biochar to soil. Biol. Fertil. Soils 48 (5), 511–517. https://doi.org/10.1007/s00374-011-0644-3.

Polverigiani, S., McCormack, M.L., Mueller, C.W., Eissenstat, D.M., 2011. Growth and physiology of olive pioneer and fibrous roots exposed to soil moisture deficits. Tree Physiol. 31 (11), 1228–1237. https://doi.org/10.1093/treephys/tpr110.

Rees, F., Watteau, F., Mathieu, S., Turpault, M., Le Brech, Y., Qiu, R., Morel, J.L., 2017. Metal immobilization on wood-derived biochars: distribution and reactivity of carbonate phases. J. Environ. Qual. 46 (4), 845–854. https://doi.org/10.2134/jeq2017.04.0152.

Sanaei, D., Sarmadi, M., Dehghani, M.H., Sharifan, H., Ribeiro, P.G., Guilherme, L.R.G., Rahimi, S., 2023. Towards engineering mitigation of leaching of Cd and Pb in co-contaminated soils using metal oxide-based aerogel composites and biochar. Environ. Sci.: Process. Impacts 25, 2110–2124. https://doi.org/10.1039/D3EM00284E, 2023.

Shapiro, S.S., Wilk, M.B., 1965. An analysis of variance test for normality (complete samples). Biometrika 52, 591–611.

Sharifan, H., Ma, X., 2021. Foliar application of zn agrichemicals affects the bioavailability of arsenic, cadmium and micronutrients to rice (Oryza sativa l.) in flooded paddy soil. Agriculture (Switzerland) 11 (6). https://doi.org/10.3390/agriculture11060505.

Simiele, M., Argentino, O., Baronti, S., Scippa, G.S., Chiatante, D., Terzaghi, M., Montagnoli, A., 2022. Biochar enhances plant growth, fruit yield, and antioxidant content of cherry tomato (Solanum lycopersicum L.) in a soilless substrate. Agriculture (Switzerland) 12 (8). https://doi.org/10.3390/agriculture12081135.

Stefanowicz, A.M., Kapusta, P., Zubek, S., Stanek, M., Woch, M.W., 2020. Soil organic matter prevails over heavy metal pollution and vegetation as a factor shaping soil microbial communities at historical Zn–Pb mining sites. Chemosphere 240. https://doi.org/10.1016/j.chemosphere.2019.124922.

Tang, J., Zhang, L., Zhang, J., Ren, L., Zhou, Y., Zheng, Y., Luo, L., Yang, Y., Huang, H., Chen, A., 2020. Physicochemical features, metal availability and enzyme activity in heavy metal-polluted soil remediated by biochar and compost. Sci. Total Environ. 701. https://doi.org/10.1016/j.scitotenv.2019.134751.

Viotti, C., Albrecht, K., Amaducci, S., Bardos, P., Bertheau, C., Blaudez, D., Bothe, L., Cazaux, D., Ferrarini, A., Govilas, J., Gusovius, H.J., Jeannin, T., Lühr, C., Müssig, J., Pilla, M., Placet, V., Puschenreiter, M., Tognacchini, A., Yung, L., Chalot, M., 2022. Nettle, a long-known fiber plant with new perspectives. In materials. MDPI 15 (Issue 12). https://doi.org/10.3390/ma15124288.

Wang, J., Zhao, M., Zhang, J., Zhao, B., Lu, X., Wei, H., 2021. Characterization and utilization of biochars derived from five invasive plant species Bidens pilosa L., Praxelis clematidea, Ipomoea cairica, Mikania micrantha and Lantana camara L. for Cd2+ and Cu2+ removal. J. Environ. Manag. 280, 111746. https://doi.org/10.1016/j.jenvman.2020.111746.

Wang, S., Du, Z., Shi, X., Chen, Y., Chen, G., 2024. Linking root traits to phytoremediation in trees and shrubs: implications of root economics spectrum. J. Appl. Ecol. 61 (2), 249–259. https://doi.org/10.1111/1365-2664.14556.

Wang, X., Zheng, W.L., Yuan, H.M., van Kleunen, M., Yu, F.H., Li, M.H., 2024. B. Biochar produced from diverse invasive species improves remediation of cadmium-contaminated soils. Biol. Invasions 26 (8), 2595–2606. https://doi.org/10.1007/s10530-024-03332-3.

Weber, K., Quicker, P., 2018. Properties of biochar. Fuel 217 (September 2017), 240–261. https://doi.org/10.1016/j.fuel.2017.12.054.

Wu, J., Fu, X., Zhao, L., Lv, J., Lv, S., Shang, J., Lv, J., Du, S., Guo, H., Ma, F., 2024. Biochar as a partner of plants and beneficial microorganisms to assist in-situ bioremediation of heavy metal contaminated soil. Sci. Total Environ. 923. https://doi.org/10.1016/j.scitotenv.2024.171442. Elsevier B.V.

Xiang, Y., Deng, Q., Duan, H., Guo, Y., 2017. Effects of biochar application on root traits: a meta-analysis. GCB Bioenergy 9, 1563–1572. https://doi.org/10.1111/gcbb.12449.

Yin, D., Wang, X., Chen, C., Peng, B., Tan, C., Li, H., 2016. Varying effect of biochar on Cd, Pb and as mobility in a multi-metal contaminated paddy soil. Chemosphere 152, 196–206. https://doi.org/10.1016/j.chemosphere.2016.01.044.